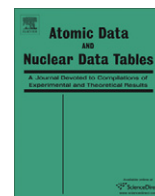




Contents lists available at ScienceDirect

## Atomic Data and Nuclear Data Tables

journal homepage: [www.elsevier.com/locate/adt](http://www.elsevier.com/locate/adt)Axial and reflection asymmetry of the nuclear ground state<sup>☆</sup>P. Möller<sup>a,\*</sup>, R. Bengtsson<sup>b</sup>, B.G. Carlsson<sup>b</sup>, P. Olivius<sup>b</sup>, T. Ichikawa<sup>c</sup>, H. Sagawa<sup>d</sup>, A. Iwamoto<sup>e</sup><sup>a</sup> Theoretical Division, Los Alamos National Laboratory, Los Alamos, NM 87545, USA<sup>b</sup> Department of Mathematical Physics, Lund Institute of Technology, P.O. Box 118, SE-22100 Lund, Sweden<sup>c</sup> RIKEN Nishina Center, RIKEN, Wako, Saitama 351-0198, Japan<sup>d</sup> Center for Mathematical Sciences, University of Aizu, Aizu-Wakamatsu, Fukushima 965-80, Japan<sup>e</sup> Japan Atomic Energy Agency (JAEA), Tokai-mura, Naka-gun, Ibaraki 319-1195, Japan

## ARTICLE INFO

## Article history:

Available online 10 July 2008

## ABSTRACT

More than a decade ago we published a calculation of nuclear ground-state masses and deformations in Atomic Data and Nuclear Data Tables [P. Möller, J.R. Nix, W.D. Myers, W.J. Swiatecki, *At. Data Nucl. Data Tables* 59 (1995) 185]. In this study, triaxial nuclear shapes were not considered. We have now enhanced our model and studied the influence of triaxial shape degrees of freedom on the nuclear ground-state potential-energy (mass) and ground-state shape. It turns out that a few hundred nuclei are affected to a varying degree with the largest effect, about 0.7 MeV, occurring near <sup>108</sup>Ru. We provide here a table of the calculated effects of triaxial shape degrees of freedom. Although axial-asymmetry effects were not considered in the 1995 mass calculation, it did study the effects of reflection-asymmetric shape degrees of freedom ( $\epsilon_3$ ) on nuclear masses. However, the magnitude of the effect was not tabulated. Here, we provide such a table. In addition we calculate the effect in a much improved fashion: we search a four-dimensional deformation space ( $\epsilon_2$ ,  $\epsilon_3$ ,  $\epsilon_4$ , and  $\epsilon_6$ ). This is now possible because the computational resources available to us today are more than 100,000 times better than at the time we calculated the mass table published in 1995.

© 2008 Elsevier Inc. All rights reserved.

<sup>☆</sup> This paper is dedicated to the memory of our friend, colleague, and collaborator George A. Leander who in the 1980s made so many important contributions to the studies of axial and reflection asymmetry in the nuclear ground state.

\* Corresponding author.

E-mail address: [moller@lanl.gov](mailto:moller@lanl.gov) (P. Möller).

## Contents

1. Introduction	759
1.1. Which minimum is the ground state?	759
2. Axial asymmetry in the nuclear ground state	760
3. Reflection asymmetry in the nuclear ground state	761
4. Discussion	761
4.1. Triaxiality in the nuclear ground state	761
4.2. Reflection asymmetry in the nuclear ground state	763
Acknowledgments	763
Appendix A	763
Appendix B	764
References	764
Explanation of Tables	765
Explanation of Graphs	766
Tables	
1. Calculated effect of axial asymmetry on nuclear ground-state masses and deformations	767
2. Calculated effect of reflection asymmetry on nuclear ground-state masses and deformations	773
Graphs	
1. Four calculated potential-energy surfaces versus $\varepsilon_2$ and $\gamma$ (minimized with respect to $\varepsilon_4$ )	777
2. Calculated ground-state axial asymmetry instability for nuclei in the range $47 < N < 143$	778
3. Calculated ground-state octupole instability for nuclei in the range $47 < N < 143$	779
4. Twelve calculated potential-energy surfaces versus $\varepsilon_2$ and $\gamma$ (minimized with respect to $\varepsilon_4$ ) for even Ru isotopes from $^{98}\text{Ru}$ to $^{120}\text{Ru}$	780

## 1. Introduction

In a previous issue of Atomic Data and Nuclear Data Tables we presented a calculation of nuclear ground-state masses and deformations for 8979 nuclei ranging from  $^{16}\text{O}$  to  $^{339}\text{136}$  and extending from the proton drip line to the neutron drip line [1]. The calculation was based on the macroscopic–microscopic approach. The microscopic corrections were obtained from levels calculated in a folded-Yukawa single-particle potential [2] by use of the Strutinsky method [3,4]. Residual pairing corrections were calculated in the Lipkin–Nogami approximation [5–8]. Two 1992 mass tables were provided, both with this microscopic correction, but with the macroscopic contribution to the total potential energy obtained in two different liquid-drop type models, namely the finite-range droplet model, and the finite-range liquid-drop model. We refer to the macroscopic–microscopic model in which the total potential energy is calculated as a sum of microscopic corrections from folded-Yukawa single-particle levels and a macroscopic energy term from the finite-range droplet model as the FRDM. The potential-energy model in which the macroscopic term is given by the finite-range liquid-drop model are referred to as the FRLDM. If present, a year in brackets refers to the year the constants and other features of a particular “edition” of the model were determined and frozen. Publication of an edition may not take place until several years later due to the lengthy publication process. For example, the FRDM (1992) appeared in print in 1995 [1].

For historical reasons and for compatibility with previous calculations we use the Nilsson perturbed-spheroid  $\epsilon$  shape parameterization. Its complete specification, including axial asymmetry, is quite lengthy and is given in our mass paper [1]. We use the FRLDM model in our calculations here. Because the calculation of fission barriers was much improved relative to the calculations used when the FRLDM (1992) parameter set was determined, we recently redetermined the FRLDM parameters [9]. This most recent model/parameter set we refer to as FRLDM (2002). It is this version that we use here. However, for the results given here the slight difference in model parameters between the FRLDM (1992) and FRLDM (2002) are unimportant for  $\Delta E_\gamma$  and  $\Delta E_\epsilon$ ; the two parameter choices give results that are very similar. The parameter differences are mainly important for fission-barrier heights.

Axial asymmetry was not implemented in the computer codes at the time of our mass paper, but this has now been accomplished. A couple of misprints relating to axial asymmetry that occur in some of the equations in Ref. [1] (but which have not migrated to any calculations) are enumerated and corrected in Appendix. We present in Table 1 the detailed results of the first global calculation of the effect of triaxiality on the nuclear ground-state shape and mass. When the calculated binding energy is affected by more than 10 keV by triaxiality we tabulate in Table 1 the magnitude of the effect and the values of the deformation parameters  $\epsilon_2$ ,  $\epsilon_4$ , and  $\gamma$ . An overview of these results has recently been presented in Ref. [10].

The effect of reflection-asymmetric shape degrees of freedom on nuclear masses was taken into account in the mass calculation presented in Ref. [1] but how much the ground-state energy was lowered by reflection-asymmetric shape degrees of freedom relative to calculations restricted to reflection-symmetric shapes was not presented in tabular form. We present in Table 2 the magnitude of the effect, determined in an improved way, from minimization of the potential energy in a full four-dimensional deformation space in the coordinates  $\epsilon_2$ ,  $\epsilon_3$ ,  $\epsilon_4$ , and  $\epsilon_6$  and the calculated values of those coordinates.

The effect  $\Delta E_\gamma$  on the ground-state potential-energy surface due to axial asymmetry is defined as the difference

$$\Delta E_\gamma = \min_{\epsilon_2, \epsilon_4} E(\epsilon_2, \epsilon_4, \gamma = 0) - \min_{\epsilon_2, \epsilon_4, \gamma} E(\epsilon_2, \epsilon_4, \gamma). \quad (1)$$

Similar definitions and considerations hold for  $\Delta E_{\epsilon_3}$ .

## 1.1. Which minimum is the ground state?

Surprisingly, for heavy nuclei it is non-trivial to determine which of the many minima in the calculated multi-dimensional potential-energy surface should represent the nuclear “ground state.” To illustrate this, let us consider a double-peaked heavy-element fission barrier. In a calculation we obtain with increasing elongation of the nuclear shape a ground-state minimum, a first barrier peak, a fission-isomeric minimum, and an outer barrier peak. For a nucleus such as  $^{238}\text{U}$ , for example, the calculated fission-isomeric minimum is 2–3 MeV higher than the ground-state minimum. However, for some heavy nuclei we may obtain a first

barrier peak 6 MeV above the first minimum, a fission-isomeric minimum with an energy 1 MeV below the first minimum and an outer barrier peak 2 MeV higher than the fission-isomeric minimum. To choose the ground state as  $\min_{\epsilon_2, \epsilon_4, \gamma} E(\epsilon_2, \epsilon_4, \gamma)$  would mean that the fission isomer would be considered the ground state and that its mass would be entered into the mass table. However, because of the low barrier this configuration would have such a short fission half-life that it would be difficult to observe. In contrast, this nucleus would have a long fission-decay half-life in the first, slightly higher minimum. It is therefore more natural to consider the first minimum as the “ground state” of this nucleus.

No ambiguity in identifying the ground-state minimum in calculated potential-energy surfaces will arise if we define the nuclear ground state as the minimum with the highest barrier with respect to fission. We are able to identify this minimum by use of immersion techniques in our calculated multi-dimensional potential-energy landscapes [11]. It is this minimum we tabulate in a mass table and use as the ground state. However, it is not possible to define  $\Delta E_\gamma$  for some nuclei with  $N \geq 160$  because it is not clear it should be defined with respect to  $\min_{\epsilon_2, \epsilon_4} E(\epsilon_2, \epsilon_4, \gamma = 0)$  for nuclei with complex potential-energy surfaces. We have checked that for nuclei with  $N < 160$  the two methods for selecting which of several minima is the ground state yield identical results, except for  $^{232}\text{No}$ . However, for this nucleus the ground-state mass is not decreased by triaxiality. Therefore, we can unambiguously define  $\Delta E_\gamma$  for the region of the nuclear chart tabulated in Table 1. For  $N \geq 160$  it is still straightforward to determine which minimum is the ground state and the corresponding nuclear ground-state mass, although it is more difficult, and in some cases impossible, to find a natural definition of  $\Delta E_\gamma$ . Therefore, we must limit the tabulation in Table 1 to nuclei with  $N < 160$ .

## 2. Axial asymmetry in the nuclear ground state

In our computer model most of the time is used to calculate the single-particle levels. Once the levels are determined the time to calculate the shell corrections and macroscopic contributions to the potential energy is almost negligible. The same set of levels can be used to calculate the shell correction for several neighboring nuclei to satisfactory accuracy. However, excursions too far away would lead to inaccuracies because the single-particle well radius changes with the size of the system and other parameters such as the spin-orbit strength also vary slowly with nuclear size.

We consider nuclei between the neutron and proton drip lines from  $A = 31$  to  $A = 330$ . We divide this region into 45 different subregions, each of which is sufficiently limited so that within each subregion the shell corrections can be calculated from the same set of single-particle levels. These subregions are defined by first selecting larger regions of the nuclear chart, namely from  $A = 31$  to  $A = 50$ ,  $A = 51$  to  $A = 70$ , and so on, with each section 20 nucleons wide. We then subdivide each of these regions into three parts: a region on the proton-rich side of  $\beta$  stability, a region corresponding to  $\beta$ -stable and near- $\beta$ -stable nuclei, and a third region consisting of neutron-rich nuclei. For each of these 45 subregions we calculate the energy for each nucleus for the deformation grid  $\epsilon_2 = (0.0, 0.025, \dots, 0.45)$ ,  $\gamma = (0.0, 2.5, \dots, 60.0)$ , and  $\epsilon_4 = (-0.12, -0.10, \dots, 0.12)$ , altogether 6175 grid points. So that we can determine, when multiple minima are present in the calculated potential-energy surfaces, which of these minima has the highest barrier with respect to fission, we extend the calculations to  $\epsilon_2 = 0.75$  for  $A > 170$ . For lighter nuclei the correct ground state is always obtained by using the simpler criterion that the lowest minimum should be designated as the ground state. In practice we calculate each subregion on a separate CPU in our computer

cluster. The three-dimensional potential-energy space of each nucleus is then analyzed by immersion techniques and all minima and all saddle points are identified.

As a final step we generate potential-energy contour plots of all systems. The contour maps have been constructed in the following way. In each point  $\epsilon_2$  and  $\gamma$  we display the lowest energy obtained for the 13  $\epsilon_4$  grid points calculated. We have previously strongly emphasized that such a procedure in general does not give reasonable results in, for example, situations where the surface contains multiple local minima versus  $\epsilon_4$  and in some other situations [11,9]. However, we use the method for the purpose of overview illustration only. All of our specific results on minima and separating saddle points are obtained from a complete and appropriate immersion analysis of the full 3D space. These data are written onto a file, which is then read by the plotting program which inserts the location of the minima and saddle points in the contour plots. The minima in the plots are shown as dots and the saddle points as X symbols. We show four representative contour plots in Graph 1. Here, we are only interested in the axially-asymmetric minima. However, other interesting situations occur. For example, oblate–prolate shape isomers and other types of shape isomers. They will be the subject of another paper.

In our calculations we use the same set of single-particle levels to calculate the shell-plus-pairing corrections for several nearby nuclei. We take one additional step to enhance accuracy after the minima and separating saddle points have been determined. The deformations and energies of all these stationary points were written by the immersion-analysis program onto a file. The energies at these deformations are then recalculated with the precise model parameters for the nucleus under consideration. Some quantities that depend on  $Z$  and  $N$  are the single-particle potential radii and depths, the strength of the spin-orbit force and the pairing strength which are all smoothly and slowly varying functions of  $Z$  and  $N$ . Thus, in the recalculation these quantities assume their exact proper values for this nucleus and the shell-plus-pairing corrections are calculated from the precise levels obtained. This strategy is based on the assumption that the locations of minima or saddles are less sensitive to parameter variations than the energy itself. We have performed numerous checks of this assumption and it is fulfilled to a very high degree. We used the same procedure to calculate the FRDM (1992) and FRLDM (1992) mass tables [1].

For nuclei whose ground states are affected by axial asymmetry, we determine how much the axial-asymmetry shape degree of freedom lowers the ground-state energy relative to the minimum energy that is obtained in calculations restricted to axial symmetry. These results are given in Table 1 and Graph 2. When reviewing the results on axial asymmetry, we observe that near  $Z = 44$  the effect of axial asymmetry changes very suddenly near  $Z + N = A = 110$ . This is exactly where we change parameters from a strip  $A = 91 \rightarrow 110$  to  $A = 111 \rightarrow 130$  and the rapid drop-off could be due to a change of parameters. Therefore, we have recalculated nuclei in this region for parameters appropriate for a strip  $A = 106 \rightarrow 115$  (so there is no discontinuity in model parameters across the  $A = 110$  line) and use that calculation in this specific region. But no significant effect on the results was observed. We still obtain an abrupt disappearance of axial asymmetry near  $A = 110$  and a reemergence near  $A = 120$ .

A suite of computer programs and scripts has been developed to perform the immersion analysis, plot the potential-energy graphs, generate the tables, and other related steps in this procedure in a highly automated fashion. For a discussion on how our results on axial asymmetry compare to experimental data we refer to the recent paper [10].

### 3. Reflection asymmetry in the nuclear ground state

In our mass calculation [1] the determination of the ground-state mass proceeded in the following way. In the initial step the potential energy was calculated as a function of  $\epsilon_2$  and  $\epsilon_4$ . The ground-state minimum was identified in this space and the values of the shape coordinates  $\epsilon_2$  and  $\epsilon_4$  were tabulated. Then, for each nucleus, two further minimizations were carried out, both with  $\epsilon_2$  and  $\epsilon_4$  held fixed at their previously determined values. In one of the minimizations the energy was minimized with respect to  $\epsilon_3$ , in the other  $\epsilon_6$  was varied (with  $\epsilon_3 = 0$ ). The lowest of the two minima obtained was tabulated as the ground state.

Here we considerably refine this calculation. In 1987, when we performed the first step in our mass calculation, namely the calculation of the potential-energy surfaces versus  $\epsilon_2$  and  $\epsilon_4$  we saved (and have retained ever since) these simple potential-energy surfaces and a table of *all* minima found in these surfaces. Here, we study the stability of all these minima in a full 4D deformation space in the coordinates  $\epsilon_2$ ,  $\epsilon_3$ ,  $\epsilon_4$  and  $\epsilon_6$ . We use a grid with a grid-point distance of 0.01 in all four deformation parameters. We start by calculating a 4D “hyper-cube” around the minimum found in the 2D  $\epsilon_2$ – $\epsilon_4$  space. Such a hyper-cube consists of 81 grid points, 80 of them on the surface of the hyper-cube. The lowest energy will be a grid point on the surface of this hyper-cube, unless the initial point determined from the limited 2D calculation accidentally turns out to be the location of the local minimum. If not, we construct a new 4D hyper-cube around the grid point corresponding to the lowest energy on the surface of the initial hyper-cube, taking care not to recalculate energies that are already calculated. We continue in this fashion until the lowest-energy point is *not* on the surface of the last hyper-cube investigated. It is then the interior point in this last hyper-cube that is the minimum in the full 4D space. We investigate all the minima found in the 2D space in this fashion. However, we find that sometimes there exists one minimum for  $\epsilon_3 = 0$  and another at  $\epsilon_3 \approx 0.1$ , separated by a low ridge. We therefore repeat the search for minima with the above starting points, except  $\epsilon_3 = 0.1$  in all the starting points. The lowest of the 4D minima is the optimum choice for the ground state.

We now do a completely analogous calculation but in a 3D space, with  $\epsilon_3$  set to zero. We identify the lowest minimum in this space. The difference between the minimum energies in the 3D and 4D spaces we tabulate as  $\Delta E_{\epsilon_3}$  in Table 2 and Graph 3.

This approach improves the accuracy of our original study for two reasons. First, in the original study we only investigated one minimum with respect to higher multipole deformations, namely the lowest minimum found in the 2D  $\epsilon_2$ – $\epsilon_4$  space. However, if another minimum, a shape isomer, exists in the 2D  $\epsilon_2$ – $\epsilon_4$  space then, if the effect of varying  $\epsilon_3$  and  $\epsilon_6$  is investigated for both these minima, it may turn out that the higher of the original minima becomes the lower minimum after the full variation of the four deformation parameters. Second, we perform a completely independent variation of the four deformation parameters in a full 4D deformation space, rather than the very restricted variation that was the only tractable computation possible more than a decade ago.

For a discussion on how our results on reflection asymmetry compare to experimental data we refer to Refs. [12–14].

### 4. Discussion

Determining the ground-state shapes of nuclei has been a very active research field for more than 50 years, ever since it became clear in the 1950s that nuclei are not always spherical in their ground states but may be oblate or prolate in shape. Later, interest expanded to other types of symmetry-breaking shapes, in particular reflection-asymmetric and triaxial ground-state shapes of nuclei. Apart from our studies there are no global studies covering

the whole nuclear chart within a consistent model framework of such effects. However, many studies of these effects in limited regions of nuclei have been performed previously in a variety of models. No consistent picture emerges from those studies, but in some of the studies there are similarities with our current results. Triaxiality in nuclei has mostly been studied in rotating nuclei. A recent review of symmetry breaking in rotating nuclei is in Ref. [15]. An extensive review of reflection asymmetry in the nuclear ground state is Ref. [16]; more limited discussions of triaxiality and reflection asymmetry in the nuclear ground state are given in Refs. [14,17,18]. Because of the availability of extensive reviews we restrict ourselves here to a discussion of how a few representative earlier calculations in limited regions of the nuclear chart compare to our current global investigation.

#### 4.1. Triaxiality in the nuclear ground state

Perhaps the first comprehensive study of axial asymmetry in the nuclear ground state over a large region of nuclei is the 1969 study of the “neutron-deficient rare-earth region,” that is  $50 < Z$ ,  $N < 82$  by Arseniev et al. [19]. They state in their conclusions “Thus, the equilibrium shapes are axially symmetric.” However, this is contrary to our current results where we find strong effects of axial asymmetry at  $N = 76$ , in agreement with experimental results and some more recent theoretical studies (see discussion in [10]). In addition they find  $^{126}\text{Ba}$  to be oblate in the ground state, whereas we find that the conditional oblate minimum is 1.5 MeV higher than the prolate ground state. These differences are probably due to unsuitable Nilsson single-particle parameters ( $\kappa$  and  $\mu$ ), the calculation of the potential energy by summing the oscillator single-particle levels, a method we now know is deficient [3,4,20,21], rather than by the Strutinsky shell correction method [3,4], and to a lesser degree, the non-consideration of hexadecapole shape degrees of freedom in [19]. A subsequent paper by the same authors [22] looks at axial asymmetry in the  $A \approx 100$  region, again with a negative result. But this paper suffers from the same deficiencies as the rare-earth region study.

Somewhat later Götz and collaborators considered triaxial shape degrees of freedom in the nuclear ground state [23–25]. In the study [24] of nuclei just “southwest” of  $^{208}\text{Pb}$ , that is nuclei with  $Z < 82$ ,  $N < 126$ , no triaxial minima are found. For W and Os this is in agreement with our findings. For  $^{194}\text{Pt}$  for which they show a contour diagram, and for which they obtain a weakly oblate ground state we obtain a triaxial ground state, as we also do for many other Pt and Au nuclei. In their later more ambitious paper [25] there is only weak evidence for triaxiality for  $^{130}\text{Cs}$ ,  $^{132}\text{Cs}$ ,  $^{128}\text{Ba}$ , and  $^{130}\text{Ba}$ . This is somewhat in contrast to our results where we find the largest effect for  $N = 76$ , not for  $N = 72$ , as is apparently obtained in [24]. For the heavier rare-earth elements the calculation does not extend sufficiently far towards the proton-rich side to include  $N = 76$ . A problem with these calculations, much discussed at the time, is the much too bound doubly-magic  $^{208}\text{Pb}$ . This “problem” has never existed in global mass calculations based on the folded-Yukawa single-particle potential [26–29].

In a study by Larsson [30] the onset of triaxiality of the nuclear ground state along a sequence of Pt isotopes, at  $^{190}\text{Pt}$  agrees with our results in Table 1, but triaxiality disappears slightly sooner, already at  $^{194}\text{Pt}$  in [30] whereas we find some effect remains until  $^{195}\text{Pt}$ .

We find in our calculations across the nuclear chart the largest effect of triaxial deformations on the energy of the nuclear ground state for  $^{108}\text{Ru}$  and nearby nuclei, that is for some nuclei in the  $A \approx 100$  region. Faessler et al. [31] considered triaxial effects on nuclei in this region. This calculation shows very interesting agreement with our results, to the extent we can compare the calculations. The calculation of Faessler et al. does not provide the magnitude of the effect of triaxiality on the nuclear ground-state



energy, nor does it sufficiently include many nuclei that we can establish how high in neutron number they find triaxial ground states for the very interesting isotope chains Mo and Ru. But when we compare our Table 1 here and their Table 2a in [31] we find substantial similarities between our results. In terms of  $Z$ , significant effects start to occur at  $Z = 42$  and above. For Mo and Ru, axial asymmetry starts to become important at  $A = 98$ – $100$  in both calculations. In our calculation there is no effect beyond  $A = 109$  for Mo and  $A = 111$  for Ru. There is again an effect of triaxiality setting in at about  $A = 116$  in our calculation. The Faessler calculation does not include these neutron-rich nuclei. For Pd we see an effect of triaxiality in the range  $107 \leq A \leq 111$ , Faessler (only even nuclei are considered) for  $A = 106, 108$ , and  $110$ .

A later study by Skalski and collaborators [18] also looks at triaxiality in the  $A \approx 100$  region near  $^{108}\text{Ru}$ . Potential-energy surfaces are calculated by the use of two different pairing models, namely a PNP (particle-number-projection) pairing model and a BCS pairing model. The results obtained in the PNP approach appear very similar to our results. For example, for  $^{108}\text{Ru}$  the decrease in potential energy due to triaxiality is about 0.7 MeV and  $\gamma = 19.9$ , in close agreement with 0.63 MeV and  $\gamma = 25.0$  in Table 1. In contrast, their results with the BCS pairing model are quite different, with little effect from triaxiality on the ground-state energy, about 0.2 MeV.

Skalski's results seem to indicate that the choice of pairing model is crucial. We have therefore calculated the decrease in ground-state mass due to triaxiality for  $^{108}\text{Ru}$  when we use our implementation of the BCS pairing model, as defined in Ref. [8] and with the constants specified there. We find a decrease due to triaxiality of 0.46 MeV, 73% of the effect found in the Lipkin–Nogami pairing model and significantly larger than found by Skalski [18]. Therefore, how crucial is the choice of pairing model?

Olofsson<sup>1</sup> and collaborators [32] have shown that the fluctuating part of the pairing energy (i.e., the pairing-correction energy) is for all practical purposes the same in the BCS and PNP models, provided that the same pairing strength is used and the pairing-correction energies for odd systems are calculated as described by Olofsson [32]. Thus, if the smooth part of the pairing energy is subtracted out and compensated for by a pairing-related term in the macroscopic energy, the choice of pairing model makes little difference for the total energy, implying that we get the same energy surfaces, masses, and odd–even mass differences. This applies also to the Lipkin–Nogami pairing model. However, the self-consistent pairing gap, calculated with the same pairing strength, depends on the pairing model, being larger in the PNP model than in the BCS model.

The often-made claim that the BCS and PNP pairing models give different results is based on a misconception, namely that the self-consistent pairing gap should be identified with the experimental odd–even mass difference and that the pairing strength should be adjusted so that the self-consistent pairing gap reproduces the experimental odd–even mass difference. Done this way a larger pairing strength is required in the BCS pairing model than in the PNP pairing model. As a result, the pairing shell energy is different in the two models, leading to differences in energy surfaces, masses, and odd–even mass differences as exemplified by Skalski's calculations.

A large number of experiments have over the years looked at the level structure of nuclei in the  $A \approx 100$  region, for example, Refs. [33–37]. In particular the later studies have very complete data for very neutron-rich Ru isotopes, up to  $^{112}\text{Ru}$ . Low-lying  $\gamma$  bands are seen in the data also in the most neutron-rich isotopes, although we obtain axially-symmetric ground states for  $^{112}\text{Ru}$  (oblate shape) as is obtained in the HFB potential-energy surface shown in Fig. 8 in the study by Åystö et al. [35], where the ground

state is prolate. In both calculations the potential is much softer in the  $\gamma$  direction for  $^{112}\text{Ru}$  than for  $^{108}\text{Ru}$ . In our calculation the triaxial ground state of  $^{108}\text{Ru}$  is much more strongly established than in the calculation of Åystö et al. [35]. We show in Graph 4 how the properties of the potential-energy surface evolve for a sequence of 12 even Ru isotopes from  $^{98}\text{Ru}$  to  $^{120}\text{Ru}$ .

Additional calculations on triaxiality of the nuclear ground state have appeared over the years but no very consistent picture emerges from these calculations which employ a variety of macroscopic–microscopic potentials or self-consistent HFB models with Skyrme forces. The lack of a consistent picture can be expected, since none of these calculations (with one exception, see below) has been benchmarked in a global calculation of nuclear masses and deformations, in contrast to the model presented here, which has been applied to global calculations in successively enhanced versions for more than 25 years [27,2,2]. However, there is one area of substantial consensus: most calculations find that triaxial shapes are important in the neutron-deficient rare-earth region with a maximum effect at  $N = 76$ , as we do here. In their early work, based on a Nilsson modified-oscillator single-particle potential, Ragnarsson and collaborators [38] find an effect at  $N = 76$  with a maximum at  $Z = 62$ – $64$ , in agreement with our results. However, hexadecapole deformations are not included in the  $\gamma$  plane in Ragnarsson's calculations. Girod and Grammaticos [39] studied six nuclei with respect to axial asymmetry in an HFB model. There is an almost complete non-overlap with their results and our results here; we only agree that  $^{134}\text{Ce}$  has a static triaxial ground-state shape. A later more extensive study was published in 1983 [40]. In their study of some proton-rich rare-earth nuclei, Redon et al. [41] find triaxial ground states in the vicinity of  $N = 76$  for Sm, but none for Cd, in qualitative agreement with our results. In a more comprehensive study Kern et al. [42] consider the behavior of light rare-earth level spectra and how they evolve in the range  $132 \leq A \leq 140$ . They find that the level spectra for some of these nuclei are best understood in terms of potential-energy surfaces with well-established triaxial minima. For these nuclei they also find that static potential-energy surfaces obtained in calculations based on their macroscopic–microscopic model with a Woods–Saxon single-particle potential exhibit such well-established triaxial ground states.

In 2000 Dutta et al. calculated ground-state shapes in the ETFSI method in an implementation that allowed triaxial nuclear shapes [43]. Earlier, this ETFSI model, restricted to axially-symmetric shapes, had been used in global calculations of nuclear ground-state masses by Aboussir et al. [44]. Since this is the only study of triaxial nuclear ground-state shapes in a microscopic model that has been benchmarked in a global nuclear mass calculation, it is of considerable interest to compare with our results. However, one should note that the study of triaxial nuclear ground-state shapes by Dutta et al. is not global, it is limited to 36 relatively randomly selected nuclei; in contrast we study almost 9000 nuclei. The authors find that out of the 36 nuclei they study 32 are triaxial in their ground states. This preponderance of triaxial ground-state shapes is unanticipated and seems to be contradicted by experimental level-structure data [10]. The authors conjecture that they obtain triaxial shapes in so many cases just as a compensation for a too limited axially-symmetric deformation space, namely only two deformation parameters ( $c, h$ ). To test this conjecture, they study what happens in their model if they release the constraint of reflection asymmetry, but retain axial symmetry. They find that in most cases the nuclei remained right–left symmetric. They summarize with the comment “We are thus inclined to accept the widespread occurrence of triaxiality that we find as being an essential feature of ETFSI calculations, if not of the real world.” In contrast, in our work about an equal number of nuclei are affected by axial and reflection asymmetry, which seems to be more consistent with real-world observations [10]. One point of similarity between our

<sup>1</sup> Olofsson is known as Uhrenholt after September 2, 2007.

results is that in the calculations by Dutta et al. [43], axial asymmetry lowers the nuclear ground state by a maximum of 0.7 MeV with respect to minima found in calculations restricted to axial symmetry, in agreement with the maximum effect we find.

#### 4.2. Reflection asymmetry in the nuclear ground state

Because of the long-known low-lying negative-parity states in nuclei near  $^{222}\text{Ra}$ , many limited theoretical studies on octupole effects have been presented previously. Early attempts to find non-zero equilibrium octupole deformations in this region of the nuclear chart were negative. Vogel calculated potential-energy surfaces by summing Nilsson modified-oscillator single-particle levels but found no instability with respect to octupole deformations [45]. In a similar study based on the same Nilsson potential, but with the potential-energy surfaces calculated by use of the just-developed macroscopic–microscopic method [3,4,20] only a few nuclei were subject to a weak octupole instability for oblate shapes [46]. Later Neergård and Vogel developed a model in which they described the low-lying negative-parity states in terms of octupole vibrations [47,48].

A turning point in the studies of octupole effects in the nuclear ground state were the results obtained in the FRLDM (1981) study of nuclear masses by Möller and Nix [12]. In this study ground-state shapes and masses were determined by minimizing the nuclear potential energy with respect to  $\epsilon_2$  and  $\epsilon_4$  shape degrees of freedom. Additional shape degrees of freedom were not taken into account due to the computational limitations at that time. It was observed that some of the largest differences between calculated and experimental nuclear ground-state masses in the nuclear chart were centered at  $^{222}\text{Ra}$  and that this correlated well with the experimental observations that the negative-parity states observed in experiments had their lowest energies near  $^{222}\text{Ra}$ . A calculation of octupole deformations on the nuclear ground state was performed for five sample nuclei, namely  $^{91}\text{Kr}$ ,  $^{184}\text{Hf}$ ,  $^{218}\text{Ra}$ ,  $^{222}\text{Ra}$ , and  $^{224}\text{Ra}$ . An effect was found only for  $^{222}\text{Ra}$  and  $^{224}\text{Ra}$  for which the consideration of octupole deformations decreased the discrepancy between calculated and experimental masses from 1.81 to 0.11 MeV and 1.43 to 0.41 MeV, respectively.

These results gave the impetus to a large number of new theoretical and experimental studies, for example [13,49] and the very comprehensive work by Leander and Chen [14], which also contains a large number of references to experimental and theoretical work. In Ref. [14], Leander and Chen modeled the low-energy spectroscopy of odd- $A$  nuclei in the mass region  $A \approx 219$ – $229$  by coupling states of a deformed shell model, including octupole deformation, to a reflection-asymmetric rotor core. In their conclusions they summarize “The description of experimental data was optimized for each nucleus with respect to  $\beta_3$ . The fact that this optimization invariably favored or allowed a non-zero  $\beta_3$  leaves little doubt about the role of some sort of surface octupole mode in the  $A \approx 219$ – $229$  region.” Furthermore, in the abstract they state “Overall agreement requires an octupole deformation of  $\beta_3 \approx 0.1$ .” Our results in Table 2 agree very well with this analysis, both in terms of where the effect occurs ( $A \approx 219$ – $229$ ) (also cf. Ref. [16]) and the magnitude of  $\beta_3$  ( $\approx 0.1$ ).

The first global nuclear-mass calculation in which octupole deformations were consistently taken into account was the nuclear-mass model/table FRLDM (1992) [1]. It led to a clear improvement in the calculated masses in the region near  $^{222}\text{Ra}$  as can be seen by comparing Fig. 1 in Ref. [29] with Fig. 1 in Ref. [1]. However, the effect of octupole shape degrees of freedom on nuclear masses was not quantified. In Ref. [10] we show that for the nuclei where we find an effect of reflection asymmetry, the calculated masses are on average too high by 1.032 MeV, when reflection asymmetry is not taken into account. When reflection asymmetry

is taken into account, the absolute value of the mean deviation  $\mu$  decreases to only 0.168 MeV.

As mentioned above, we have performed a more accurate calculation of reflection asymmetry in the nuclear ground state. In the previous studies we only looked for octupole effects on the nuclear ground state if the minimum found in  $(\epsilon_2, \epsilon_4)$  space was unstable with respect to small deviations from reflection symmetry. This restriction was due to the computational limitations at the time. We have now established that sometimes a lower minimum is found for reflection-asymmetric shapes for some nuclei even if the reflection-symmetric minimum is stable with respect to small octupole deformations. That is, two minima exist, one reflection symmetric and one reflection asymmetric, and they are separated by a saddle. Another improvement in the current study is that the reflection-symmetric minimum is determined in a full 3D minimization in  $(\epsilon_2, \epsilon_4, \epsilon_6)$  space and the reflection-asymmetric minimum in a full 4D minimization in  $(\epsilon_2, \epsilon_3, \epsilon_4, \epsilon_6)$  space. The effect of the improvements is that we find that the region beyond Pb where we obtain reflection-asymmetric ground states extends slightly further in neutron number  $N$ . For example, for Th we find an effect for  $N = 136, 137$ , and  $138$ , whereas in the FRLDM (1992) Table [1] the effect of the octupole degree of freedom only extends to  $N = 135$ . The situation is similar for other actinide isotope chains.

#### Acknowledgments

We are grateful to Arnold Sierk for many discussions during the course of this investigation and for a careful reading of the final manuscript. Comments by Henrik Uhrenholt<sup>2</sup> on the PNP and BCS pairing models are highly appreciated. This work was carried out under the auspices of the National Nuclear Security Administration of the US Department of Energy at Los Alamos National Laboratory under Contract No. DE-AC52-06NA25396. This work was also supported by a travel grant to JUSTIPEN (Japan-US Theory Institute for Physics with Exotic Nuclei) under Grant No. DE-FG02-06ER41407 (U. Tennessee).

#### Appendix A

In our 1995 mass paper [1] and in a related paper [50] a number of misprints occurred. They have not migrated into any calculation. For completeness we give the corrected equations here. The equation numbers refer to the equation numbers in the original papers. Eq. (20) in [1] should read

$$v = \cos 2\phi_t = \frac{\xi^2 - \eta^2}{\xi^2 + \eta^2} = \frac{[1 + \frac{1}{3}\epsilon_2 \cos \gamma] \cos 2\phi + (\frac{1}{3})^{1/2} \epsilon_2 \sin \gamma}{1 + \frac{1}{3}\epsilon_2 \cos \gamma + (\frac{1}{3})^{1/2} \epsilon_2 \sin \gamma \cos 2\phi}.$$

This also applies to Eq. (33) in [50].

Eq. (33) in [1], middle line, should read

$$SY_{44} = \sqrt{\frac{315}{128\pi}} \sin^4 \theta \cos 4\phi = \sqrt{\frac{315}{128\pi}} (1 - u^2)^2 (2v^2 - 1).$$

This also applies to Eq. (A.10) in the appendix of Ref. [50], middle line.

A related equation in Appendix of Ref. [50], Eq. (A.17) third line is missing a factor 2 and should read

$$\frac{\partial SY_{44}}{\partial u} = -\sqrt{\frac{315}{128\pi}} 4u(1 - u^2)(2v^2 - 1).$$

<sup>2</sup> Uhrenholt was known as Olofsson before September 2, 2007.

## Appendix B. Supplementary data

Supplementary data associated with this article can be found, in the online version, at [doi:10.1016/j.adt.2008.05.002](https://doi.org/10.1016/j.adt.2008.05.002).

## References

- [1] P. Möller, J.R. Nix, W.D. Myers, W.J. Swiatecki, *At. Data Nucl. Data Tables* 59 (1995) 185.
- [2] M. Bolsterli, E.O. Fiset, J.R. Nix, J.L. Norton, *Phys. Rev. C* 5 (1972) 1050.
- [3] V.M. Strutinsky, *Nucl. Phys. A* 95 (1967) 420.
- [4] V.M. Strutinsky, *Nucl. Phys. A* 122 (1968) 1.
- [5] H.J. Lipkin, *Ann. Phys. (NY)* 9 (1960) 272.
- [6] Y. Nogami, *Phys. Rev.* 134 (1964) B313.
- [7] H.C. Pradhan, Y. Nogami, J. Law, *Nucl. Phys. A* 201 (1973) 357.
- [8] P. Möller, J.R. Nix, *Nucl. Phys. A* 536 (1992) 20.
- [9] P. Möller, A.J. Sierk, A. Iwamoto, *Phys. Rev. Lett.* 92 (2004) 072501.
- [10] P. Möller, R. Bengtsson, B.G. Carlsson, P. Olivius, T. Ichikawa, *Phys. Rev. Lett.* 97 (2006) 162502.
- [11] P. Möller, D.G. Madland, A.J. Sierk, A. Iwamoto, *Nature* 409 (2001) 785.
- [12] P. Möller, J.R. Nix, *Nucl. Phys. A* 361 (1981) 117.
- [13] G.A. Leander, R.K. Sheline, P. Möller, P. Olanders, I. Ragnarsson, A.J. Sierk, *Nucl. Phys. A* 388 (1982) 452.
- [14] G.A. Leander, Y.S. Chen, *Phys. Rev. C* 37 (1988) 2744.
- [15] S. Frauendorf, *Rev. Mod. Phys.* 73 (2001) 463.
- [16] P.A. Butler, W. Nazarewicz, *Rev. Mod. Phys.* 68 (1996) 349.
- [17] S. Åberg, H. Flocard, W. Nazarewicz, *Ann. Rev. Nucl. Sci.* 40 (1990) 439.
- [18] J. Skalski, S. Mizutori, W. Nazarewicz, *Nucl. Phys. A* 617 (1997) 282.
- [19] D.A. Arseniev, A. Sobieczewski, V.G. Soloviev, *Nucl. Phys. A* 126 (1969) 15.
- [20] S.G. Nilsson, C.F. Tsang, A. Sobieczewski, Z. Szymański, S. Wycech, C. Gustafson, I.-L. Lamm, P. Möller, B. Nilsson, *Nucl. Phys. A* 131 (1969) 1.
- [21] P. Möller, *Nucl. Phys. A* 192 (1972) 529.
- [22] D.A. Arseniev, A. Sobieczewski, V.G. Soloviev, *Nucl. Phys. A* 139 (1969) 269.
- [23] U. Götz, H.C. Pauli, K. Alder, *Nucl. Phys. A* 175 (1971) 481.
- [24] U. Götz, H.C. Pauli, K. Junker, *Phys. Lett.* 39B (1972) 436.
- [25] U. Götz, H.C. Pauli, K. Alder, K. Junker, *Nucl. Phys. A* 192 (1972) 1.
- [26] P. Möller, S.G. Nilsson, J.R. Nix, *Nucl. Phys. A* 229 (1974) 292.
- [27] P. Möller, J.R. Nix, *At. Data Nucl. Data Tables* 26 (1981) 165.
- [28] P. Möller, J.R. Nix, *At. Data Nucl. Data Tables* 39 (1988) 213.
- [29] P. Möller, W.D. Myers, W.J. Swiatecki, J. Treiner, *At. Data Nucl. Data Tables* 39 (1988) 225.
- [30] S.E. Larsson, *Phys. Scr.* 8 (1973) 17.
- [31] A. Faessler, J.E. Galonska, U. Götz, H.C. Pauli, *Nucl. Phys. A* 230 (1974) 302.
- [32] H. Olofsson, R. Bengtsson, P. Möller, *Nucl. Phys. A* 784 (2007) 104.
- [33] F.K. McGowan, R.L. Robinson, P.H. Stelson, W.T. Milner, *Nucl. Phys. A* 113 (1968) 529.
- [34] N. Kaffrell, N. Trautmann, G. Hermann, H. Ahrens, *Phys. Rev. C* 8 (1973) 320.
- [35] J. Äystö, P.P. Jauho, Z. Janas, A. Jokinen, J.M. Parmonen, H. Penttilä, P. Taskinen, R. Béraud, R. Duffait, A. Emsallem, J. Meyer, M. Meyer, N. Redon, M.E. Leino, K. Eskola, P. Dendooven, *Nucl. Phys. A* 515 (1990) 365.
- [36] J.A. Shannon, W.R. Phillips, J.L. Durell, B.J. Varley, W. Urban, C.J. Pearson, I. Ahmad, C.J. Lister, L.R. Morss, K.L. Nash, C.W. Williams, N. Schulz, E. Lubkiewicz, M. Bentaleb, *Phys. Lett. B* 336 (1994) 136.
- [37] S.J. Zhu, Y.X. Luo, J.H. Hamilton, A.V. Ramayya, X.L. Che, Z. Jiang, J.K. Hwang, J.L. Wood, M.A. Stoyer, R. Donangelo, J.D. Cole, C. Goodin, J.O. Rasmussen, *Eur. Phys. J. A*, submitted for publication.
- [38] I. Ragnarsson, A. Sobieczewski, R.K. Sheline, S.E. Larsson, B. Nerlo-Pomorska, *Nucl. Phys. A* 233 (1974) 329.
- [39] M. Girod, B. Grammaticos, *Phys. Rev. Lett.* 40 (1978) 361.
- [40] M. Girod, B. Grammaticos, *Phys. Rev. C* 27 (1983) 2317.
- [41] N. Redon, J. Meyer, M. Meyer, P. Quentin, P. Bonche, H. Flocard, P.-H. Heenen, *Phys. Rev. C* 38 (1988) 550.
- [42] B.D. Kern, R.L. Mlekodaj, G.A. Leander, M.O. Kortelahti, E.F. Zganjar, R.A. Braga, R.W. Fink, C.P. Perez, W. Nazarewicz, P.B. Semmes, *Phys. Rev. C* 36 (1987) 1514.
- [43] A.K. Dutta, J.M. Pearson, F. Tondeur, *Phys. Rev. C* 61 (2000) 054303.
- [44] Y. Aboussir, J.M. Pearson, A.K. Dutta, F. Tondeur, *At. Data Nucl. Data Tables* 61 (1995) 127.
- [45] P. Vogel, *Nucl. Phys. A* 112 (1968) 583.
- [46] P. Möller, S.G. Nilsson, R.K. Sheline, *Phys. Lett.* 40B (1972) 329.
- [47] K. Neergård, P. Vogel, *Nucl. Phys. A* 145 (1970) 33.
- [48] K. Neergård, P. Vogel, *Nucl. Phys. A* 149 (1970) 217.
- [49] W. Nazarewicz, P. Olanders, I. Ragnarsson, J. Dudek, G.A. Leander, P. Möller, E. Ruchowska, *Nucl. Phys. A* 429 (1984) 269.
- [50] P. Möller, A. Iwamoto, *Nucl. Phys. A* 575 (1994) 381.

## Explanation of Tables

**Table 1. Calculated effect of axial asymmetry on nuclear ground-state masses and deformations**

- Z** Proton number. The table is ordered by increasing proton number. The corresponding chemical symbol of each named element is given in parentheses
- N** Neutron number
- A** Mass number
- $\epsilon_2$  Calculated ground-state quadrupole deformation in the Nilsson perturbed-spheroid parameterization
- $\epsilon_4$  Calculated ground-state hexadecapole deformation in the Nilsson perturbed-spheroid parameterization
- $\gamma$  Calculated ground-state gamma deformation in the Nilsson perturbed-spheroid parameterization
- $\Delta E_\gamma$  Calculated decrease in potential energy due to triaxiality. We only present nuclei for which the calculated decrease in energy due to triaxiality is equal to or larger than 0.01 MeV

**Table 2. Calculated effect of reflection asymmetry on nuclear ground-state masses and deformations**

- Z** Proton number. The table is ordered by increasing proton number. The corresponding chemical symbol of each named element is given in parentheses
- N** Neutron number
- A** Mass number
- $\epsilon_2$  Calculated ground-state quadrupole deformation in the Nilsson perturbed-spheroid parameterization
- $\epsilon_3$  Calculated ground-state octupole deformation in the Nilsson perturbed-spheroid parameterization
- $\epsilon_4$  Calculated ground-state hexadecapole deformation in the Nilsson perturbed-spheroid parameterization
- $\epsilon_6$  Calculated ground-state hexacontatetrapole deformation in the Nilsson perturbed-spheroid parameterization
- $\Delta E_{\epsilon_3}$  Calculated decrease in potential energy due to reflection asymmetry
- We only present nuclei for which the calculated decrease in energy due to reflection asymmetry is equal to or larger than 0.01 MeV. In contrast to the calculation leading to our FRDM (1992) mass table [1] the ground-state determination here is based on calculations in a full 4D space. The accuracy of the calculation is 0.005 in each of the four deformation parameters



## Explanation of Graphs

### Graph 1. Four calculated potential-energy surfaces versus $\epsilon_2$ and $\gamma$ (minimized with respect to $\epsilon_4$ )

Minima are indicated by colored round dots, saddle points by pairs of crossed lines. The numbers on the background give the energy in MeV of the thicker contour lines which are spaced 1 MeV apart; the spacing between the thinner lines is 0.2 MeV. For the Th diagram the intervals are doubled. To obtain a suitable range of values in the plotted surfaces we have, following standard practice, subtracted the energy obtained for a spherical shape in the macroscopic part of the model. This normalization has the additional advantage that the ground-state mass can be obtained as the sum of the energy of the minimum in the plot and the macroscopic energy of the nucleus for a spherical shape. The surfaces exhibit typical structures that we obtain in our current investigation. Each point in a surface corresponds to the energy of a specific nuclear shape. The lower left tip of the pie-like plot corresponds to a spherical shape. Points along the upper straight line correspond to oblate shapes (like a discus) and those along the lower straight line to prolate shapes (like an American football). The energy values in the interior of the pie are calculated for axially-asymmetric nuclear shapes (a somewhat simplified analogy is that these points correspond to shapes that result from standing on a football). Shapes corresponding to the three minima and one of the saddle points of  $^{216}\text{Th}$  are shown at the top. Shapes at equivalent locations in the other plots are similar, but not exactly identical, due to possible differences in the  $\epsilon_4$  shape coordinate. In subplot (3)  $^{216}\text{Th}$  exhibits triple shape coexistence. The lowest minimum is spherical, the next higher one oblate, and finally there is a triaxial minimum, close to the prolate axis. Our immersion-analysis program has identified as optimum saddle points between pairs of minima the locations indicated by the crossed-lines symbols.

### Graph 2. Calculated ground-state axial asymmetry instability for nuclei in the range $47 < N < 143$

Although Table 1 extends over a larger region of the nuclear chart we limit the region displayed to regions where significant effects are found. Because we have recently increased the number of integration points in some calculations in our computer codes there are some (insignificant) differences between this Graph and the Figure published in Ref. [10]. How our results relate to experimental data is discussed in Ref. [10].

### Graph 3. Calculated ground-state octupole instability for nuclei in the range $47 < N < 143$

Although Table 2 extends over a larger region of the nuclear chart we limit the region displayed to regions where significant effects are found. Our calculations here are much more detailed than were possible in our mass paper published in 1995. Therefore, there are some fairly significant differences between the calculated data in this Graph and Fig. 14 in Ref. [1]. The main difference is that for actinide nuclei the calculated region of octupole instability extends about three neutrons further away from  $N = 126$  than in [1].

### Graph 4. Twelve calculated potential-energy surfaces versus $\epsilon_2$ and $\gamma$ (minimized with respect to $\epsilon_4$ ) for even Ru isotopes from $^{98}\text{Ru}$ to $^{120}\text{Ru}$

The Ru isotopes from  $^{100}\text{Ru}$  to  $^{110}\text{Ru}$  are triaxial in shape. A less well-established triaxiality reemerges at  $^{116}\text{Ru}$  but gradually fades away as  $N = 82$  is approached. For  $^{112}\text{Ru}$  and  $^{114}\text{Ru}$  the potential-energy surfaces are quite soft in the  $\gamma$  direction. If two minima are present the saddle between the minima is indicated by crossed lines, but only if the saddle is at least 0.05 MeV higher than the higher of the two minima, as is the case for  $^{112}\text{Ru}$ . For  $^{114}\text{Ru}$  the saddle at  $\epsilon_2 = 0.25, \gamma = 20.0$  is less than 0.05 MeV above the prolate minimum at  $\epsilon_2 = 0.25, \gamma = 0.0$ . Therefore, the saddle and the prolate minimum are not marked.

**Table 1**

Calculated effect of axial asymmetry on nuclear ground-state masses and deformations. See page 765 for Explanation of Tables

<i>N</i>	<i>A</i>	$\epsilon_2$	$\epsilon_4$	$\gamma$	$\Delta E_\gamma$ (MeV)
<i>Z</i> = 9( <i>F</i> )					
27	36	0.225	−0.12	40.0	0.03
<i>Z</i> = 11( <i>Na</i> )					
31	42	0.275	0.04	32.5	0.21
<i>Z</i> = 12( <i>Mg</i> )					
30	42	0.275	0.06	32.5	0.03
31	43	0.275	0.04	32.5	0.29
32	44	0.225	0.04	30.0	0.11
35	47	0.225	0.04	30.0	0.30
<i>Z</i> = 13( <i>Al</i> )					
26	39	0.275	−0.08	37.5	0.04
27	40	0.300	−0.10	47.5	0.15
28	41	0.325	−0.12	57.5	0.02
29	42	0.275	−0.10	55.0	0.03
30	43	0.275	−0.06	55.0	0.03
31	44	0.250	0.00	50.0	0.14
32	45	0.125	0.00	32.5	0.07
33	46	0.125	0.02	32.5	0.02
35	48	0.175	0.02	30.0	0.07
36	49	0.175	0.02	30.0	0.04
<i>Z</i> = 14( <i>Si</i> )					
26	40	0.275	−0.08	42.5	0.03
33	47	0.125	0.00	40.0	0.04
<i>Z</i> = 15( <i>P</i> )					
27	42	0.275	−0.06	50.0	0.08
30	45	0.250	0.00	55.0	0.03
31	46	0.125	0.02	35.0	0.05
32	47	0.125	0.02	32.5	0.02
35	50	0.175	0.04	42.5	0.03
<i>Z</i> = 16( <i>S</i> )					
16	32	0.250	0.12	32.5	0.01
17	33	0.250	0.10	45.0	0.03
29	45	0.250	0.00	57.5	0.01
31	47	0.225	0.06	50.0	0.13
41	57	0.350	0.08	30.0	0.22
42	58	0.350	0.08	30.0	0.31
43	59	0.325	0.08	30.0	0.19
<i>Z</i> = 17( <i>Cl</i> )					
26	43	0.175	0.04	15.0	0.03
27	44	0.250	0.02	47.5	0.02
29	46	0.200	0.04	55.0	0.02
30	47	0.200	0.06	52.5	0.04
31	48	0.225	0.08	55.0	0.08
32	49	0.175	0.08	55.0	0.03
33	50	0.175	0.06	45.0	0.09
37	54	0.225	0.10	55.0	0.02
42	59	0.250	0.10	55.0	0.01
43	60	0.275	0.06	30.0	0.36
44	61	0.275	0.06	30.0	0.09
46	63	0.175	0.02	10.0	0.03
<i>Z</i> = 18( <i>Ar</i> )					
27	45	0.100	0.02	30.0	0.03
47	65	0.175	0.02	15.0	0.02
49	67	0.100	0.02	32.5	0.06
<i>Z</i> = 19( <i>K</i> )					
27	46	0.075	0.00	27.5	0.01
45	64	0.125	−0.02	10.0	0.02
46	65	0.125	0.00	12.5	0.02
47	66	0.125	0.02	15.0	0.02
48	67	0.100	0.02	32.5	0.05
49	68	0.100	0.00	37.5	0.02
<i>Z</i> = 24( <i>Cr</i> )					
18	42	0.150	0.02	32.5	0.03
<i>Z</i> = 25( <i>Mn</i> )					
18	43	0.200	0.02	32.5	0.04
63	88	0.300	−0.02	7.5	0.04
64	89	0.300	−0.02	7.5	0.02
<i>Z</i> = 26( <i>Fe</i> )					
17	43	0.225	0.06	32.5	0.08
19	45	0.100	0.00	30.0	0.02
<i>Z</i> = 27( <i>Co</i> )					
17	44	0.250	0.02	47.5	0.05
18	45	0.250	0.02	52.5	0.01
19	46	0.100	0.02	30.0	0.05
37	64	0.100	0.02	42.5	0.04

**Table 1 (continued)**

<i>N</i>	<i>A</i>	$\epsilon_2$	$\epsilon_4$	$\gamma$	$\Delta E_\gamma$ (MeV)
41	68	0.050	0.00	27.5	0.02
56	83	0.050	0.00	22.5	0.02
59	86	0.050	0.00	22.5	0.02
67	94	0.300	0.04	2.5	0.02
<i>Z</i> = 28( <i>Ni</i> )					
27	55	0.025	0.00	35.0	0.02
<i>Z</i> = 29( <i>Cu</i> )					
35	64	0.125	0.02	17.5	0.02
57	86	0.100	−0.02	32.5	0.17
59	88	0.100	−0.02	32.5	0.20
65	94	0.300	0.02	10.0	0.05
<i>Z</i> = 30( <i>Zn</i> )					
36	66	0.150	0.02	30.0	0.01
64	94	0.300	0.02	12.5	0.02
65	95	0.300	0.02	12.5	0.09
73	103	0.225	0.04	22.5	0.11
74	104	0.200	0.02	25.0	0.25
75	105	0.200	0.04	30.0	0.13
<i>Z</i> = 31( <i>Ga</i> )					
30	61	0.150	−0.02	10.0	0.03
31	62	0.200	0.00	32.5	0.05
32	63	0.200	0.02	32.5	0.06
36	67	0.175	0.02	32.5	0.03
37	68	0.175	0.02	45.0	0.03
38	69	0.175	0.02	45.0	0.02
41	72	0.200	0.02	40.0	0.08
42	73	0.200	0.02	35.0	0.17
43	74	0.125	−0.02	12.5	0.01
51	82	0.100	−0.02	32.5	0.07
52	83	0.125	−0.02	20.0	0.03
53	84	0.125	−0.02	15.0	0.05
54	85	0.150	−0.02	15.0	0.09
55	86	0.175	0.00	15.0	0.05
56	87	0.175	0.00	12.5	0.03
60	91	0.225	0.02	20.0	0.11
63	94	0.275	0.00	17.5	0.13
64	95	0.275	0.02	17.5	0.22
65	96	0.275	0.02	17.5	0.25
66	97	0.275	0.02	17.5	0.19
67	98	0.275	0.04	10.0	0.08
73	104	0.225	0.04	22.5	0.17
74	105	0.200	0.04	27.5	0.38
75	106	0.200	0.04	30.0	0.38
<i>Z</i> = 32( <i>Ge</i> )					
31	63	0.200	0.02	22.5	0.03
32	64	0.225	0.02	32.5	0.07
37	69	0.225	0.04	42.5	0.07
38	70	0.225	0.04	40.0	0.04
41	73	0.225	0.04	42.5	0.07
42	74	0.225	0.04	40.0	0.18
43	75	0.250	0.04	35.0	0.38
60	92	0.225	0.02	20.0	0.07
63	95	0.275	0.02	20.0	0.09
64	96	0.275	0.02	20.0	0.21
65	97	0.300	0.02	20.0	0.25
66	98	0.300	0.02	22.5	0.15
67	99	0.275	0.04	10.0	0.04
73	105	0.225	0.06	22.5	0.15
74	106	0.200	0.04	27.5	0.35
75	107	0.200	0.04	30.0	0.40
76	108	0.200	0.04	30.0	0.15
77	109	0.150	0.04	25.0	0.08
<i>Z</i> = 33( <i>As</i> )					
43	76	0.250	0.04	45.0	0.04
51	84	0.125	0.02	7.5	0.03
61	94	0.300	−0.04	7.5	0.03
62	95	0.300	−0.02	10.0	0.03
63	96	0.300	0.00	17.5	0.14
64	97	0.300	0.00	20.0	0.25
65	98	0.300	0.02	20.0	0.25
66	99	0.300	0.02	22.5	0.11
67	100	0.275	0.06	7.5	0.02
73	106	0.200	0.06	7.5	0.03
74	107	0.200	0.06	22.5	0.15
<i>Z</i> = 33( <i>As</i> )					
75	108	0.200	0.06	25.0	0.26

(continued on next page)

Table 1 (continued)

<i>N</i>	<i>A</i>	$\epsilon_2$	$\epsilon_4$	$\gamma$	$\Delta E_\gamma$ (MeV)
76	109	0.175	0.06	25.0	0.05
77	110	0.150	0.04	20.0	0.06
<i>Z</i> = 34( <i>Se</i> )					
63	97	0.325	0.00	17.5	0.12
64	98	0.325	0.00	20.0	0.21
65	99	0.325	0.02	20.0	0.27
66	100	0.325	0.02	20.0	0.03
73	107	0.225	0.08	12.5	0.02
74	108	0.200	0.06	17.5	0.04
75	109	0.200	0.06	25.0	0.18
76	110	0.175	0.06	22.5	0.13
77	111	0.150	0.06	20.0	0.03
<i>Z</i> = 35( <i>Br</i> )					
63	98	0.325	0.00	15.0	0.07
64	99	0.325	0.00	17.5	0.14
65	100	0.325	0.02	17.5	0.19
73	108	0.225	0.06	7.5	0.04
74	109	0.200	0.06	30.0	0.10
75	110	0.200	0.06	30.0	0.39
76	111	0.175	0.06	30.0	0.26
77	112	0.150	0.06	32.5	0.21
<i>Z</i> = 36( <i>Kr</i> )					
52	88	0.075	0.00	52.5	0.08
64	100	0.325	0.02	10.0	0.03
65	101	0.325	0.02	12.5	0.07
74	110	0.200	0.06	27.5	0.15
75	111	0.200	0.06	30.0	0.27
76	112	0.150	0.06	35.0	0.13
77	113	0.150	0.06	37.5	0.11
78	114	0.100	0.02	2.5	0.03
<i>Z</i> = 37( <i>Rb</i> )					
31	68	0.250	0.02	47.5	0.08
32	69	0.275	0.04	50.0	0.07
33	70	0.275	0.04	55.0	0.03
43	80	0.250	0.06	55.0	0.02
44	81	0.250	0.06	52.5	0.04
52	89	0.075	0.00	47.5	0.02
54	91	0.150	0.00	42.5	0.01
74	111	0.200	0.06	30.0	0.18
75	112	0.200	0.06	30.0	0.06
76	113	0.150	0.06	45.0	0.06
77	114	0.150	0.06	45.0	0.05
89	126	0.100	0.00	30.0	0.11
90	127	0.100	0.00	30.0	0.02
<i>Z</i> = 38( <i>Sr</i> )					
31	69	0.275	0.04	40.0	0.04
32	70	0.275	0.04	40.0	0.12
43	81	0.325	0.04	12.5	0.07
<i>Z</i> = 39( <i>Y</i> )					
31	70	0.275	0.02	5.0	0.01
55	94	0.200	0.00	42.5	0.08
<i>Z</i> = 40( <i>Zr</i> )					
32	72	0.275	0.04	35.0	0.27
55	95	0.175	0.00	37.5	0.12
74	114	0.175	0.06	57.5	0.08
<i>Z</i> = 41( <i>Nb</i> )					
54	95	0.175	0.00	35.0	0.09
55	96	0.200	0.00	37.5	0.19
56	97	0.200	0.00	30.0	0.12
57	98	0.225	0.02	22.5	0.04
65	106	0.325	0.04	15.0	0.15
66	107	0.325	0.06	15.0	0.16
67	108	0.300	0.06	7.5	0.02
73	114	0.200	0.06	50.0	0.03
96	137	0.275	−0.02	7.5	0.01
<i>Z</i> = 42( <i>Mo</i> )					
35	77	0.275	0.06	57.5	0.03
54	96	0.175	0.00	32.5	0.09
55	97	0.200	0.00	32.5	0.12
56	98	0.200	0.00	27.5	0.16
57	99	0.225	0.02	27.5	0.27
58	100	0.225	0.02	25.0	0.15
63	105	0.300	0.02	17.5	0.11
64	106	0.300	0.02	17.5	0.26
65	107	0.325	0.04	20.0	0.30
66	108	0.300	0.04	17.5	0.30
67	109	0.300	0.06	15.0	0.04

Table 1 (continued)

<i>N</i>	<i>A</i>	$\epsilon_2$	$\epsilon_4$	$\gamma$	$\Delta E_\gamma$ (MeV)
73	115	0.200	0.06	50.0	0.06
74	116	0.200	0.06	42.5	0.10
95	137	0.250	−0.04	10.0	0.08
96	138	0.250	−0.04	12.5	0.08
97	139	0.275	−0.02	15.0	0.11
98	140	0.275	0.00	7.5	0.01
<i>Z</i> = 43( <i>Tc</i> )					
54	97	0.175	−0.02	22.5	0.02
55	98	0.175	0.00	20.0	0.06
56	99	0.200	0.00	27.5	0.12
57	100	0.225	0.02	30.0	0.26
58	101	0.225	0.02	27.5	0.27
59	102	0.225	0.02	27.5	0.26
60	103	0.275	0.02	25.0	0.20
61	104	0.275	0.02	25.0	0.20
62	105	0.275	0.02	22.5	0.31
63	106	0.300	0.02	20.0	0.42
64	107	0.300	0.04	22.5	0.52
65	108	0.300	0.04	22.5	0.59
66	109	0.300	0.04	20.0	0.49
67	110	0.300	0.06	20.0	0.23
68	111	0.275	0.06	15.0	0.04
72	115	0.225	0.06	52.5	0.02
73	116	0.225	0.06	42.5	0.23
74	117	0.200	0.06	42.5	0.26
75	118	0.200	0.06	40.0	0.23
76	119	0.175	0.06	45.0	0.10
89	132	0.125	−0.04	5.0	0.02
95	138	0.250	−0.04	12.5	0.12
96	139	0.250	−0.02	12.5	0.11
97	140	0.275	−0.02	15.0	0.12
98	141	0.275	0.00	15.0	0.11
99	142	0.275	0.00	7.5	0.02
<i>Z</i> = 44( <i>Ru</i> )					
37	81	0.250	0.06	47.5	0.05
38	82	0.225	0.08	52.5	0.01
44	88	0.250	0.06	37.5	0.03
45	89	0.250	0.06	37.5	0.02
57	101	0.200	0.02	22.5	0.11
58	102	0.225	0.04	27.5	0.18
59	103	0.225	0.04	27.5	0.32
60	104	0.250	0.04	27.5	0.38
61	105	0.250	0.04	27.5	0.35
62	106	0.250	0.04	27.5	0.41
63	107	0.275	0.04	25.0	0.57
64	108	0.275	0.04	25.0	0.63
65	109	0.275	0.04	22.5	0.67
66	110	0.275	0.04	22.5	0.47
67	111	0.275	0.04	25.0	0.22
72	116	0.225	0.06	45.0	0.07
73	117	0.225	0.06	42.5	0.27
74	118	0.200	0.06	37.5	0.28
75	119	0.200	0.06	40.0	0.35
76	120	0.150	0.06	50.0	0.02
95	139	0.225	−0.04	10.0	0.05
96	140	0.250	−0.02	15.0	0.16
97	141	0.250	−0.02	15.0	0.16
98	142	0.250	−0.02	15.0	0.12
99	143	0.275	0.00	12.5	0.05
104	148	0.275	0.04	12.5	0.03
105	149	0.275	0.04	17.5	0.21
106	150	0.275	0.04	32.5	0.31
<i>Z</i> = 45( <i>Rh</i> )					
38	83	0.250	0.08	45.0	0.05
39	84	0.250	0.08	45.0	0.04
41	86	0.225	0.08	50.0	0.03
43	88	0.250	0.06	40.0	0.05
44	89	0.250	0.06	37.5	0.08
59	104	0.225	0.04	27.5	0.17
60	105	0.225	0.04	27.5	0.35
<i>Z</i> = 45( <i>Rh</i> )					
61	106	0.250	0.04	30.0	0.44
62	107	0.250	0.04	27.5	0.51
63	108	0.250	0.04	27.5	0.56
64	109	0.275	0.04	25.0	0.65
65	110	0.275	0.04	25.0	0.62

Table 1 (continued)

N	A	$\epsilon_2$	$\epsilon_4$	$\gamma$	$\Delta E_\gamma$ (MeV)
66	111	0.275	0.04	25.0	0.33
67	112	0.275	0.04	27.5	0.11
72	117	0.225	0.06	45.0	0.10
73	118	0.225	0.06	40.0	0.31
74	119	0.200	0.06	35.0	0.36
75	120	0.200	0.06	35.0	0.37
76	121	0.175	0.06	40.0	0.16
77	122	0.150	0.06	45.0	0.01
95	140	0.225	−0.04	7.5	0.01
96	141	0.250	−0.02	12.5	0.03
97	142	0.250	−0.02	12.5	0.11
98	143	0.275	−0.02	15.0	0.08
99	144	0.275	0.00	12.5	0.06
100	145	0.275	0.00	12.5	0.02
104	149	0.275	0.04	15.0	0.06
105	150	0.275	0.04	32.5	0.05
106	151	0.250	0.06	15.0	0.25
107	152	0.250	0.06	17.5	0.37
108	153	0.250	0.06	17.5	0.38
Z = 46(Pd)					
43	89	0.250	0.08	45.0	0.04
61	107	0.225	0.04	27.5	0.11
62	108	0.225	0.04	27.5	0.24
63	109	0.250	0.04	27.5	0.31
64	110	0.250	0.04	27.5	0.32
65	111	0.275	0.04	25.0	0.27
72	118	0.225	0.06	47.5	0.04
73	119	0.225	0.06	42.5	0.20
74	120	0.200	0.06	37.5	0.22
75	121	0.175	0.06	30.0	0.20
76	122	0.150	0.06	37.5	0.07
97	143	0.250	−0.02	12.5	0.08
98	144	0.250	−0.02	12.5	0.05
104	150	0.275	0.04	15.0	0.03
105	151	0.250	0.04	10.0	0.08
106	152	0.250	0.06	15.0	0.19
107	153	0.250	0.06	17.5	0.29
108	154	0.250	0.06	17.5	0.24
109	155	0.250	0.08	20.0	0.24
110	156	0.225	0.08	17.5	0.16
Z = 47(Ag)					
73	120	0.175	0.04	30.0	0.09
74	121	0.175	0.06	30.0	0.05
75	122	0.150	0.04	30.0	0.09
105	152	0.250	0.04	7.5	0.02
106	153	0.250	0.04	12.5	0.05
107	154	0.250	0.06	15.0	0.07
108	155	0.225	0.06	7.5	0.04
Z = 48(Cd)					
73	121	0.125	0.02	20.0	0.01
Z = 49(In)					
65	114	0.100	0.00	47.5	0.02
68	117	0.100	0.00	47.5	0.01
69	118	0.100	0.02	47.5	0.02
70	119	0.100	0.02	45.0	0.04
71	120	0.100	0.02	42.5	0.04
72	121	0.100	0.02	40.0	0.05
73	122	0.100	0.02	32.5	0.07
75	124	0.100	0.04	47.5	0.01
Z = 50(Sn)					
119	169	0.100	0.04	25.0	0.07
Z = 51(Sb)					
114	165	0.150	0.02	40.0	0.04
116	167	0.100	0.02	30.0	0.01
118	169	0.100	0.02	30.0	0.07
119	170	0.100	0.02	30.0	0.13
120	171	0.075	0.02	30.0	0.14
Z = 52(Te)					
73	125	0.125	0.02	47.5	0.05
114	166	0.150	0.02	30.0	0.12
115	167	0.150	0.02	35.0	0.12
119	171	0.100	0.04	15.0	0.03
120	172	0.075	0.02	25.0	0.07
Z = 53(I)					
53	106	0.125	−0.06	12.5	0.03
54	107	0.125	−0.06	10.0	0.03
56	109	0.150	−0.04	10.0	0.02

Table 1 (continued)

N	A	$\epsilon_2$	$\epsilon_4$	$\gamma$	$\Delta E_\gamma$ (MeV)
57	110	0.150	−0.04	10.0	0.05
59	112	0.175	−0.02	5.0	0.01
62	115	0.200	−0.02	10.0	0.04
63	116	0.200	−0.02	10.0	0.05
64	117	0.200	−0.02	10.0	0.07
65	118	0.225	0.00	10.0	0.06
66	119	0.225	0.00	10.0	0.05
72	125	0.175	0.00	30.0	0.08
73	126	0.150	0.00	25.0	0.12
74	127	0.150	0.00	27.5	0.10
75	128	0.150	0.02	30.0	0.11
79	132	0.050	0.00	42.5	0.04
89	142	0.125	−0.04	7.5	0.04
93	146	0.150	−0.06	7.5	0.07
114	167	0.175	0.02	35.0	0.04
115	168	0.175	0.02	40.0	0.05
116	169	0.150	0.02	40.0	0.09
119	172	0.100	0.04	15.0	0.01
120	173	0.100	0.02	30.0	0.09
121	174	0.075	0.02	30.0	0.13
Z = 54(Xe)					
53	107	0.125	−0.06	7.5	0.01
63	117	0.225	−0.02	7.5	0.01
64	118	0.225	−0.02	10.0	0.04
65	119	0.225	0.00	7.5	0.01
73	127	0.175	0.00	22.5	0.05
74	128	0.175	0.00	25.0	0.05
75	129	0.175	0.02	27.5	0.14
76	130	0.150	0.02	30.0	0.13
79	133	0.050	0.00	42.5	0.04
120	174	0.100	0.02	30.0	0.08
121	175	0.100	0.02	30.0	0.10
Z = 55(Cs)					
63	118	0.250	−0.02	10.0	0.04
64	119	0.250	−0.02	15.0	0.08
65	120	0.250	0.00	12.5	0.03
74	129	0.175	0.02	17.5	0.05
75	130	0.175	0.02	22.5	0.19
76	131	0.150	0.02	27.5	0.18
77	132	0.150	0.02	27.5	0.11
79	134	0.075	0.00	32.5	0.06
98	153	0.225	−0.04	2.5	0.04
120	175	0.100	0.04	12.5	0.02
121	176	0.100	0.04	30.0	0.11
122	177	0.075	0.02	30.0	0.04
Z = 56(Ba)					
57	113	0.225	−0.08	7.5	0.01
64	120	0.275	−0.02	15.0	0.07
65	121	0.275	−0.02	15.0	0.03
75	131	0.175	0.02	20.0	0.09
76	132	0.150	0.02	20.0	0.11
77	133	0.150	0.02	25.0	0.17
78	134	0.125	0.02	30.0	0.12
79	135	0.100	0.02	32.5	0.12
120	176	0.100	0.04	12.5	0.01
121	177	0.100	0.04	30.0	0.17
122	178	0.075	0.02	30.0	0.08
Z = 57(La)					
63	120	0.275	−0.04	5.0	0.02
64	121	0.275	−0.02	10.0	0.07
65	122	0.275	−0.02	10.0	0.12
66	123	0.275	0.00	7.5	0.02
74	131	0.200	0.02	17.5	0.11
75	132	0.175	0.02	25.0	0.13
76	133	0.175	0.02	25.0	0.24
Z = 58(Ce)					
77	134	0.150	0.02	25.0	0.24
78	135	0.125	0.02	27.5	0.14
79	136	0.100	0.02	32.5	0.06
121	178	0.100	0.04	30.0	0.17
122	179	0.100	0.02	30.0	0.13
75	133	0.175	0.04	15.0	0.06
76	134	0.175	0.04	22.5	0.24
77	135	0.175	0.04	25.0	0.21
78	136	0.150	0.02	27.5	0.14

(continued on next page)

Table 1 (continued)

<i>N</i>	<i>A</i>	$\epsilon_2$	$\epsilon_4$	$\gamma$	$\Delta E_\gamma$ (MeV)
79	137	0.125	0.02	22.5	0.14
80	138	0.050	0.00	15.0	0.01
121	179	0.100	0.04	27.5	0.15
122	180	0.100	0.02	30.0	0.15
<i>Z</i> = 59( <i>Pr</i> )					
75	134	0.200	0.04	22.5	0.19
76	135	0.175	0.04	22.5	0.22
77	136	0.175	0.04	25.0	0.30
78	137	0.150	0.04	30.0	0.23
79	138	0.125	0.02	17.5	0.12
121	180	0.100	0.04	27.5	0.12
122	181	0.100	0.02	30.0	0.13
<i>Z</i> = 60( <i>Nd</i> )					
75	135	0.200	0.04	20.0	0.15
76	136	0.200	0.04	25.0	0.29
77	137	0.175	0.04	25.0	0.38
78	138	0.150	0.04	30.0	0.33
79	139	0.150	0.04	40.0	0.16
121	181	0.100	0.04	25.0	0.05
122	182	0.100	0.02	30.0	0.13
<i>Z</i> = 61( <i>Pm</i> )					
74	135	0.225	0.04	17.5	0.03
75	136	0.200	0.04	20.0	0.17
76	137	0.200	0.04	25.0	0.38
77	138	0.175	0.04	25.0	0.45
78	139	0.175	0.04	30.0	0.44
79	140	0.150	0.04	35.0	0.27
119	180	0.150	0.04	17.5	0.06
122	183	0.100	0.02	30.0	0.10
<i>Z</i> = 62( <i>Sm</i> )					
74	136	0.225	0.04	17.5	0.07
75	137	0.225	0.04	22.5	0.14
76	138	0.200	0.04	22.5	0.33
77	139	0.200	0.04	27.5	0.48
78	140	0.175	0.04	30.0	0.49
79	141	0.150	0.04	40.0	0.19
119	181	0.150	0.06	15.0	0.02
122	184	0.100	0.02	30.0	0.02
<i>Z</i> = 63( <i>Eu</i> )					
66	129	0.300	0.02	10.0	0.03
75	138	0.225	0.04	22.5	0.23
76	139	0.200	0.04	22.5	0.30
77	140	0.200	0.04	25.0	0.52
78	141	0.175	0.04	30.0	0.52
79	142	0.175	0.04	37.5	0.18
119	182	0.175	0.02	55.0	0.03
<i>Z</i> = 64( <i>Gd</i> )					
65	129	0.325	0.02	15.0	0.03
66	130	0.325	0.04	15.0	0.01
75	139	0.225	0.04	20.0	0.16
76	140	0.200	0.04	20.0	0.25
77	141	0.200	0.04	25.0	0.48
78	142	0.175	0.04	30.0	0.37
79	143	0.175	0.04	42.5	0.06
85	149	0.125	−0.04	5.0	0.05
119	183	0.175	0.02	57.5	0.01
<i>Z</i> = 65( <i>Tb</i> )					
65	130	0.325	0.04	17.5	0.16
66	131	0.300	0.04	12.5	0.16
67	132	0.300	0.04	10.0	0.08
75	140	0.225	0.04	17.5	0.14
76	141	0.225	0.04	22.5	0.27
77	142	0.200	0.04	22.5	0.45
78	143	0.200	0.04	25.0	0.31
79	144	0.175	0.04	45.0	0.08
<i>Z</i> = 66( <i>Dy</i> )					
67	133	0.300	0.06	10.0	0.08
75	141	0.225	0.06	15.0	0.06
76	142	0.225	0.06	20.0	0.19
77	143	0.200	0.04	20.0	0.33
78	144	0.200	0.04	25.0	0.08
79	145	0.175	0.04	52.5	0.03
<i>Z</i> = 67( <i>Ho</i> )					
76	143	0.225	0.06	17.5	0.15
77	144	0.225	0.06	20.0	0.21
78	145	0.200	0.04	22.5	0.05

Table 1 (continued)

<i>N</i>	<i>A</i>	$\epsilon_2$	$\epsilon_4$	$\gamma$	$\Delta E_\gamma$ (MeV)
79	146	0.175	0.04	52.5	0.01
85	152	0.125	−0.04	10.0	0.02
<i>Z</i> = 68( <i>Er</i> )					
77	145	0.200	0.06	12.5	0.13
79	147	0.175	0.04	55.0	0.02
119	187	0.200	0.04	57.5	0.01
<i>Z</i> = 69( <i>Tm</i> )					
77	146	0.200	0.06	10.0	0.07
<i>Z</i> = 70( <i>Yb</i> )					
77	147	0.200	0.08	7.5	0.05
<i>Z</i> = 71( <i>Lu</i> )					
77	148	0.200	0.08	7.5	0.05
79	150	0.175	0.04	55.0	0.01
123	194	0.100	0.02	57.5	0.01
129	200	0.025	0.00	30.0	0.02
<i>Z</i> = 72( <i>Hf</i> )					
77	149	0.175	0.06	17.5	0.10
79	151	0.150	0.04	52.5	0.02
83	155	0.050	0.00	22.5	0.02
<i>Z</i> = 73( <i>Ta</i> )					
78	151	0.175	0.04	45.0	0.04
79	152	0.150	0.04	47.5	0.05
<i>Z</i> = 74( <i>W</i> )					
84	158	0.075	0.00	10.0	0.04
<i>Z</i> = 75( <i>Re</i> )					
83	158	0.050	0.00	22.5	0.01
123	198	0.075	0.02	50.0	0.02
127	202	0.025	0.00	30.0	0.02
<i>Z</i> = 77( <i>Ir</i> )					
93	170	0.150	0.02	12.5	0.03
115	192	0.150	0.06	17.5	0.06
<i>Z</i> = 78( <i>Pt</i> )					
89	167	0.125	0.00	30.0	0.01
90	168	0.125	0.00	22.5	0.05
91	169	0.125	0.00	20.0	0.03
92	170	0.125	0.00	17.5	0.02
93	171	0.125	0.00	15.0	0.05
94	172	0.125	0.02	15.0	0.03
95	173	0.150	0.02	20.0	0.12
96	174	0.150	0.02	20.0	0.10
97	175	0.150	0.02	20.0	0.10
109	187	0.175	0.06	7.5	0.03
110	188	0.175	0.06	10.0	0.02
111	189	0.175	0.06	15.0	0.08
112	190	0.150	0.04	25.0	0.23
113	191	0.150	0.04	27.5	0.27
114	192	0.150	0.04	30.0	0.30
115	193	0.150	0.04	30.0	0.21
116	194	0.125	0.04	27.5	0.15
117	195	0.125	0.04	27.5	0.21
<i>Z</i> = 79( <i>Au</i> )					
89	168	0.100	0.02	52.5	0.01
90	169	0.100	0.02	52.5	0.02
92	171	0.100	0.02	35.0	0.05
93	172	0.125	0.02	32.5	0.21
94	173	0.125	0.02	32.5	0.27
95	174	0.125	0.02	32.5	0.23
96	175	0.125	0.02	30.0	0.25
97	176	0.150	0.02	32.5	0.33
98	177	0.150	0.02	32.5	0.35
99	178	0.150	0.02	30.0	0.31
117	195	0.125	0.04	27.5	0.21
<i>Z</i> = 79( <i>Au</i> )					
101	180	0.150	0.02	27.5	0.10
102	181	0.150	0.02	27.5	0.15
104	183	0.175	0.04	17.5	0.08
106	185	0.175	0.04	12.5	0.04
107	186	0.175	0.04	10.0	0.03
108	187	0.175	0.04	17.5	0.05
109	188	0.150	0.04	17.5	0.13
110	189	0.150	0.04	27.5	0.12
111	190	0.150	0.04	27.5	0.21
112	191	0.125	0.04	30.0	0.23
113	192	0.125	0.04	30.0	0.34
114	193	0.125	0.04	30.0	0.29
115	194	0.125	0.04	30.0	0.26
116	195	0.125	0.04	30.0	0.09



Table 1 (continued)

N	A	$\epsilon_2$	$\epsilon_4$	$\gamma$	$\Delta E_\gamma$ (MeV)
117	196	0.125	0.02	47.5	0.03
137	216	0.100	−0.02	12.5	0.04
Z = 80(Hg)					
96	176	0.125	0.02	40.0	0.06
97	177	0.125	0.02	40.0	0.13
98	178	0.125	0.02	40.0	0.07
99	179	0.125	0.02	42.5	0.07
Z = 81(Tl)					
92	173	0.050	0.00	30.0	0.02
97	178	0.050	0.00	12.5	0.02
99	180	0.050	0.00	30.0	0.04
158	239	0.175	0.04	12.5	0.05
Z = 82(Pb)					
155	237	0.225	0.02	7.5	0.01
156	238	0.200	0.02	12.5	0.03
157	239	0.200	0.02	15.0	0.07
158	240	0.175	0.02	15.0	0.11
159	241	0.175	0.04	12.5	0.03
Z = 83(Bi)					
111	194	0.075	0.00	17.5	0.02
112	195	0.050	0.00	30.0	0.02
113	196	0.050	0.00	27.5	0.03
114	197	0.050	0.00	30.0	0.01
156	239	0.200	0.02	15.0	0.13
157	240	0.200	0.02	15.0	0.09
158	241	0.175	0.02	17.5	0.11
159	242	0.175	0.02	17.5	0.06
160	243	0.175	0.04	12.5	0.02
Z = 84(Po)					
97	181	0.225	−0.04	17.5	0.15
98	182	0.275	−0.02	12.5	0.06
155	239	0.225	0.02	10.0	0.05
156	240	0.200	0.02	12.5	0.07
157	241	0.200	0.02	15.0	0.13
158	242	0.200	0.02	20.0	0.06
159	243	0.200	0.04	15.0	0.04
Z = 85(At)					
114	199	0.100	0.00	20.0	0.02
115	200	0.100	0.00	22.5	0.02
116	201	0.075	0.00	30.0	0.03
143	228	0.175	−0.06	7.5	0.02
155	240	0.225	0.02	12.5	0.07
156	241	0.200	0.02	15.0	0.14
157	242	0.200	0.02	17.5	0.15
158	243	0.200	0.02	20.0	0.10
159	244	0.200	0.02	22.5	0.05
Z = 86(Rn)					
107	193	0.250	0.02	15.0	0.12
116	202	0.100	0.00	30.0	0.04
117	203	0.100	0.00	30.0	0.02
154	240	0.225	0.00	10.0	0.04
155	241	0.225	0.02	12.5	0.08
156	242	0.225	0.02	15.0	0.12
157	243	0.200	0.02	15.0	0.16
158	244	0.200	0.02	17.5	0.14
159	245	0.200	0.02	20.0	0.08
160	246	0.200	0.04	15.0	0.02
Z = 87(Fr)					
111	198	0.225	0.00	55.0	0.01
115	202	0.200	0.02	52.5	0.02
117	204	0.125	0.00	50.0	0.04
154	241	0.225	0.00	10.0	0.04
155	242	0.225	0.02	12.5	0.10
156	243	0.225	0.02	17.5	0.17
157	244	0.225	0.02	17.5	0.20
158	245	0.200	0.02	17.5	0.21
159	246	0.200	0.02	17.5	0.14
160	247	0.200	0.04	15.0	0.06
Z = 88(Ra)					
109	197	0.250	0.04	20.0	0.11
110	198	0.250	0.00	47.5	0.09
111	199	0.225	0.00	45.0	0.09
112	200	0.225	0.00	47.5	0.07
113	201	0.225	0.02	45.0	0.11
114	202	0.225	0.02	47.5	0.09
115	203	0.200	0.02	45.0	0.13
117	205	0.200	0.02	52.5	0.03

Table 1 (continued)

N	A	$\epsilon_2$	$\epsilon_4$	$\gamma$	$\Delta E_\gamma$ (MeV)
154	242	0.225	0.00	10.0	0.02
155	243	0.225	0.00	12.5	0.09
156	244	0.225	0.02	15.0	0.17
157	245	0.225	0.02	17.5	0.23
158	246	0.225	0.02	20.0	0.18
159	247	0.200	0.02	17.5	0.14
160	248	0.200	0.04	12.5	0.04
Z = 89(Ac)					
107	196	0.250	0.02	15.0	0.10
108	197	0.250	0.02	17.5	0.12
109	198	0.250	0.04	17.5	0.09
110	199	0.250	0.00	45.0	0.12
111	200	0.250	0.00	47.5	0.27
112	201	0.225	0.00	42.5	0.26
113	202	0.225	0.02	42.5	0.35
114	203	0.225	0.02	42.5	0.28
115	204	0.225	0.04	45.0	0.21
116	205	0.200	0.02	45.0	0.08
117	206	0.200	0.04	52.5	0.04
155	244	0.225	0.00	12.5	0.08
156	245	0.225	0.02	15.0	0.17
157	246	0.225	0.02	17.5	0.31
158	247	0.225	0.02	20.0	0.24
159	248	0.225	0.02	22.5	0.15
160	249	0.200	0.02	15.0	0.05
Z = 90(Th)					
108	198	0.250	0.02	15.0	0.26
109	199	0.250	0.04	17.5	0.20
110	200	0.250	0.04	20.0	0.09
111	201	0.225	0.02	27.5	0.24
112	202	0.225	0.02	35.0	0.34
113	203	0.225	0.02	37.5	0.38
114	204	0.225	0.02	40.0	0.40
115	205	0.225	0.04	42.5	0.32
116	206	0.225	0.04	45.0	0.15
117	207	0.200	0.04	50.0	0.08
123	213	0.075	0.02	55.0	0.01
155	245	0.225	0.00	10.0	0.06
156	246	0.225	0.02	12.5	0.14
157	247	0.225	0.02	15.0	0.26
158	248	0.225	0.02	17.5	0.21
159	249	0.225	0.02	20.0	0.11
160	250	0.225	0.04	20.0	0.02
Z = 91(Pa)					
109	200	0.275	0.02	15.0	0.23
110	201	0.300	0.02	12.5	0.16
111	202	0.325	0.02	15.0	0.24
112	203	0.225	0.02	30.0	0.23
113	204	0.225	0.02	35.0	0.38
114	205	0.225	0.02	37.5	0.40
115	206	0.225	0.04	40.0	0.32
116	207	0.225	0.04	42.5	0.31
117	208	0.200	0.04	47.5	0.16
123	214	0.075	0.02	52.5	0.01
155	246	0.225	0.00	10.0	0.04
156	247	0.225	0.00	12.5	0.12
157	248	0.225	0.02	15.0	0.23
Z = 92(U)					
158	249	0.225	0.02	17.5	0.22
159	250	0.225	0.02	17.5	0.11
160	251	0.225	0.04	17.5	0.07
Z = 93(Np)					
111	203	0.300	0.02	15.0	0.25
112	204	0.325	0.02	17.5	0.11
113	205	0.225	0.02	30.0	0.22
114	206	0.225	0.04	37.5	0.36
115	207	0.225	0.04	37.5	0.24
116	208	0.225	0.04	40.0	0.19
117	209	0.225	0.06	47.5	0.05
123	215	0.075	0.02	52.5	0.02
156	248	0.225	0.00	10.0	0.06
157	249	0.225	0.02	12.5	0.16
158	250	0.225	0.02	15.0	0.24
159	251	0.225	0.02	17.5	0.05
113	206	0.250	0.04	35.0	0.08

(continued on next page)

Table 1 (continued)

<i>N</i>	<i>A</i>	$\epsilon_2$	$\epsilon_4$	$\gamma$	$\Delta E_\gamma$ (MeV)
114	207	0.250	0.04	37.5	0.15
115	208	0.225	0.04	37.5	0.24
116	209	0.225	0.04	40.0	0.14
117	210	0.150	0.00	7.5	0.02
119	212	0.175	0.02	55.0	0.02
156	249	0.225	0.00	7.5	0.03
157	250	0.225	0.02	12.5	0.13
158	251	0.225	0.02	15.0	0.24
159	252	0.225	0.02	15.0	0.08
160	253	0.225	0.04	15.0	0.02
<i>Z</i> = 94( <i>Pu</i> )					
115	209	0.175	0.00	15.0	0.08
116	210	0.225	0.04	37.5	0.03
117	211	0.150	0.02	5.0	0.02
157	251	0.225	0.02	10.0	0.05
158	252	0.225	0.02	12.5	0.10
<i>Z</i> = 95( <i>Am</i> )					
117	212	0.150	0.02	5.0	0.02
121	216	0.125	0.02	52.5	0.01
123	218	0.100	0.02	52.5	0.02
131	226	0.350	0.02	25.0	0.08
156	251	0.225	0.02	5.0	0.02
157	252	0.225	0.02	7.5	0.05
158	253	0.225	0.02	10.0	0.08
<i>Z</i> = 96( <i>Cm</i> )					
123	219	0.100	0.02	52.5	0.02
130	226	0.350	0.02	25.0	0.40
131	227	0.350	0.02	25.0	0.31
<i>Z</i> = 97( <i>Bk</i> )					
121	218	0.125	0.02	47.5	0.05
122	219	0.125	0.02	47.5	0.04
123	220	0.100	0.02	50.0	0.02
129	226	0.350	0.02	25.0	0.53
130	227	0.350	0.02	25.0	0.35
131	228	0.350	0.02	25.0	0.37
132	229	0.325	0.02	22.5	0.26
133	230	0.325	0.02	20.0	0.18
<i>Z</i> = 98( <i>Cf</i> )					
123	221	0.100	0.02	50.0	0.02
129	227	0.325	0.02	25.0	0.31
130	228	0.350	0.02	25.0	0.29
131	229	0.350	0.02	25.0	0.35
132	230	0.325	0.02	22.5	0.37
133	231	0.325	0.02	20.0	0.38
134	232	0.325	0.02	20.0	0.27
135	233	0.300	0.02	17.5	0.10
136	234	0.300	0.02	20.0	0.06
138	236	0.300	0.02	22.5	0.01
141	239	0.225	−0.04	5.0	0.02
<i>Z</i> = 99( <i>Es</i> )					
132	231	0.325	0.02	25.0	0.05
133	232	0.325	0.02	27.5	0.02
134	233	0.325	0.02	25.0	0.02
136	235	0.300	0.02	25.0	0.04
137	236	0.225	−0.04	10.0	0.11
138	237	0.225	−0.04	10.0	0.09
139	238	0.225	−0.04	10.0	0.07
140	239	0.225	−0.04	7.5	0.04
141	240	0.225	−0.04	5.0	0.03
<i>Z</i> = 100( <i>Fm</i> )					
136	236	0.250	−0.02	12.5	0.08
137	237	0.250	−0.02	15.0	0.16
138	238	0.250	−0.02	12.5	0.21
139	239	0.250	−0.02	12.5	0.24
140	240	0.250	−0.02	12.5	0.06
141	241	0.225	−0.02	5.0	0.01
<i>Z</i> = 101( <i>Md</i> )					
136	237	0.250	−0.02	15.0	0.05
137	238	0.250	−0.02	15.0	0.16
138	239	0.250	−0.02	15.0	0.18
139	240	0.250	−0.02	15.0	0.25
140	241	0.225	−0.02	10.0	0.07
141	242	0.225	−0.02	7.5	0.03
<i>Z</i> = 102( <i>No</i> )					
137	239	0.250	0.00	15.0	0.04
138	240	0.250	0.00	15.0	0.18

Table 1 (continued)

<i>N</i>	<i>A</i>	$\epsilon_2$	$\epsilon_4$	$\gamma$	$\Delta E_\gamma$ (MeV)
139	241	0.250	−0.02	15.0	0.23
140	242	0.225	−0.02	7.5	0.03
141	243	0.225	−0.02	7.5	0.03
<i>Z</i> = 103( <i>Lr</i> )					
138	241	0.250	0.00	15.0	0.17
139	242	0.250	0.00	15.0	0.25
140	243	0.250	0.00	15.0	0.15
141	244	0.250	0.00	15.0	0.07
<i>Z</i> = 104( <i>Rf</i> )					
138	242	0.250	0.00	15.0	0.18
139	243	0.250	0.00	15.0	0.26
140	244	0.250	0.00	15.0	0.16
141	245	0.250	0.00	15.0	0.10
<i>Z</i> = 105( <i>Db</i> )					
138	243	0.250	0.00	15.0	0.03
139	244	0.250	0.00	15.0	0.14
140	245	0.225	0.00	10.0	0.07
141	246	0.225	0.00	5.0	0.01
<i>Z</i> = 106( <i>Sg</i> )					
139	245	0.250	0.02	12.5	0.07
140	246	0.250	0.02	12.5	0.13
141	247	0.250	0.02	12.5	0.09
<i>Z</i> = 107( <i>Ns</i> )					
140	247	0.250	0.02	12.5	0.11
141	248	0.250	0.02	12.5	0.17
142	249	0.250	0.02	12.5	0.02
<i>Z</i> = 108( <i>Hs</i> )					
142	250	0.225	0.02	7.5	0.03

**Table 2**

Calculated effect of reflection asymmetry on nuclear ground-state masses and deformations. See page 765 for Explanation of Tables

<i>N</i>	<i>A</i>	$\epsilon_2$	$\epsilon_3$	$\epsilon_4$	$\epsilon_6$	$\Delta E_{\epsilon_3}$ (MeV)
<i>Z</i> = 8( <i>O</i> )						
8	16	−0.03	0.20	0.12	−0.02	0.08
<i>Z</i> = 15( <i>P</i> )						
8	23	−0.02	0.02	0.12	−0.03	0.01
<i>Z</i> = 17( <i>Cl</i> )						
8	25	−0.05	0.13	0.02	0.00	0.03
<i>Z</i> = 19( <i>K</i> )						
16	35	−0.03	0.02	0.00	−0.04	0.01
41	60	−0.07	0.07	0.00	0.00	0.03
43	62	−0.08	0.05	0.02	0.00	0.02
<i>Z</i> = 20( <i>Ca</i> )						
36	56	−0.07	0.02	0.02	0.02	0.04
37	57	−0.07	0.03	0.01	0.00	0.02
39	59	0.00	0.05	0.00	0.00	0.01
40	60	0.00	0.07	0.00	0.00	0.03
41	61	−0.02	0.09	0.00	0.00	0.05
<i>Z</i> = 21( <i>Sc</i> )						
38	59	−0.07	0.03	0.01	0.01	0.01
39	60	−0.04	0.06	0.00	0.00	0.02
40	61	−0.02	0.08	0.00	0.00	0.03
41	62	−0.04	0.09	−0.01	0.00	0.06
<i>Z</i> = 36( <i>Kr</i> )						
87	123	0.08	0.05	0.00	0.00	0.02
88	124	0.10	0.07	0.00	0.00	0.12
<i>Z</i> = 37( <i>Rb</i> )						
87	124	0.08	0.07	0.00	0.00	0.05
88	125	0.09	0.08	0.00	0.00	0.19
89	126	0.11	0.09	−0.01	0.00	0.54
90	127	0.11	0.09	−0.02	0.00	0.43
<i>Z</i> = 38( <i>Sr</i> )						
87	125	0.05	0.07	0.00	0.00	0.03
88	126	0.07	0.09	−0.01	0.00	0.17
89	127	0.10	0.10	−0.02	0.00	0.41
90	128	0.10	0.10	−0.02	0.01	0.59
<i>Z</i> = 39( <i>Y</i> )						
87	126	0.03	0.07	−0.01	0.00	0.04
88	127	0.04	0.09	−0.01	0.01	0.20
89	128	0.04	0.11	−0.01	0.01	0.51
90	129	0.04	0.12	−0.01	0.02	0.61
91	130	0.09	0.13	−0.03	0.01	0.24
<i>Z</i> = 40( <i>Zr</i> )						
88	128	0.03	0.09	−0.01	0.01	0.13
89	129	0.03	0.11	−0.01	0.01	0.45
90	130	0.03	0.12	−0.01	0.02	0.54
91	131	0.04	0.13	−0.02	0.01	0.16
<i>Z</i> = 41( <i>Nb</i> )						
87	128	0.03	0.05	−0.01	0.00	0.07
88	129	0.03	0.07	−0.01	0.00	0.13
89	130	0.01	0.11	−0.01	0.02	0.26
90	131	0.00	0.12	−0.02	0.02	0.02
<i>Z</i> = 42( <i>Mo</i> )						
89	131	0.02	0.09	−0.01	0.02	0.22
90	132	0.00	0.10	−0.01	0.01	0.11
<i>Z</i> = 43( <i>Tc</i> )						
89	132	0.03	0.08	0.00	0.01	0.08
<i>Z</i> = 44( <i>Ru</i> )						
89	133	0.11	0.03	−0.03	0.00	0.13
<i>Z</i> = 45( <i>Rh</i> )						
89	134	0.11	0.02	−0.03	0.00	0.19
<i>Z</i> = 48( <i>Cd</i> )						
42	90	−0.01	0.04	0.00	0.00	0.04
<i>Z</i> = 53( <i>I</i> )						
55	108	0.14	0.05	−0.05	0.02	0.04
56	109	0.15	0.06	−0.04	0.02	0.06
57	110	0.16	0.06	−0.03	0.02	0.12
58	111	0.16	0.06	−0.03	0.02	0.06
59	112	0.17	0.04	−0.03	0.02	0.05
90	143	0.14	0.06	−0.05	0.01	0.02
91	144	0.14	0.07	−0.05	0.01	0.01
<i>Z</i> = 54( <i>Xe</i> )						
54	108	0.15	0.05	−0.05	0.02	0.05
55	109	0.15	0.07	−0.04	0.02	0.14
56	110	0.16	0.07	−0.04	0.03	0.20
57	111	0.17	0.08	−0.03	0.03	0.23
58	112	0.18	0.07	−0.03	0.03	0.14

**Table 2 (continued)**

<i>N</i>	<i>A</i>	$\epsilon_2$	$\epsilon_3$	$\epsilon_4$	$\epsilon_6$	$\Delta E_{\epsilon_3}$ (MeV)
59	113	0.19	0.06	−0.03	0.03	0.10
87	141	0.12	0.04	−0.05	0.00	0.03
88	142	0.13	0.06	−0.06	0.01	0.11
89	143	0.14	0.08	−0.05	0.01	0.18
90	144	0.15	0.07	−0.05	0.02	0.11
91	145	0.16	0.08	−0.05	0.02	0.11
<i>Z</i> = 55( <i>Cs</i> )						
52	107	0.12	0.04	−0.05	0.01	0.01
53	108	0.15	0.07	−0.05	0.02	0.13
54	109	0.16	0.08	−0.05	0.03	0.26
55	110	0.16	0.09	−0.04	0.03	0.39
56	111	0.17	0.09	−0.04	0.03	0.41
57	112	0.18	0.09	−0.03	0.03	0.41
58	113	0.19	0.09	−0.03	0.03	0.30
59	114	0.21	0.07	−0.04	0.03	0.12
85	140	0.09	0.03	−0.04	−0.01	0.01
86	141	0.11	0.04	−0.05	0.00	0.06
87	142	0.13	0.07	−0.05	0.01	0.20
88	143	0.14	0.08	−0.06	0.01	0.35
89	144	0.15	0.09	−0.05	0.02	0.49
90	145	0.15	0.08	−0.05	0.02	0.40
91	146	0.16	0.09	−0.05	0.02	0.24
92	147	0.19	0.04	−0.07	0.01	0.02
<i>Z</i> = 56( <i>Ba</i> )						
52	108	0.13	0.05	−0.05	0.01	0.05
53	109	0.15	0.08	−0.05	0.02	0.21
54	110	0.17	0.09	−0.04	0.03	0.34
55	111	0.17	0.10	−0.04	0.03	0.47
56	112	0.18	0.10	−0.03	0.04	0.48
57	113	0.19	0.10	−0.03	0.04	0.44
58	114	0.20	0.09	−0.03	0.04	0.31
85	141	0.09	0.05	−0.04	0.00	0.04
86	142	0.12	0.06	−0.05	0.01	0.14
87	143	0.14	0.08	−0.05	0.01	0.35
88	144	0.15	0.09	−0.05	0.02	0.49
89	145	0.16	0.10	−0.05	0.02	0.57
90	146	0.16	0.09	−0.05	0.02	0.47
91	147	0.17	0.09	−0.05	0.03	0.12
131	187	0.10	0.06	−0.05	0.00	0.11
132	188	0.11	0.08	−0.05	0.00	0.29
133	189	0.11	0.09	−0.06	0.01	0.64
<i>Z</i> = 57( <i>La</i> )						
53	110	0.17	0.06	−0.05	0.02	0.14
54	111	0.18	0.09	−0.04	0.03	0.24
55	112	0.18	0.10	−0.04	0.04	0.35
56	113	0.20	0.10	−0.03	0.04	0.38
57	114	0.21	0.08	−0.05	0.04	0.24
58	115	0.24	0.05	−0.06	0.02	0.02
85	142	0.10	0.06	−0.03	0.00	0.15
86	143	0.12	0.08	−0.04	0.00	0.21
87	144	0.14	0.09	−0.05	0.01	0.41
88	145	0.16	0.09	−0.05	0.02	0.53
89	146	0.16	0.10	−0.04	0.02	0.48
90	147	0.17	0.09	−0.05	0.02	0.32
91	148	0.21	0.02	−0.08	0.01	0.01
131	188	0.10	0.07	−0.04	0.00	0.28
132	189	0.11	0.08	−0.05	0.00	0.48
133	190	0.11	0.09	−0.05	0.00	0.76
134	191	0.13	0.10	−0.05	0.01	0.76
135	192	0.14	0.10	−0.06	0.02	0.54
<i>Z</i> = 58( <i>Ce</i> )						
55	113	0.20	0.08	−0.04	0.04	0.31
56	114	0.21	0.08	−0.03	0.04	0.21
85	143	0.12	0.06	−0.03	0.00	0.14
86	144	0.13	0.07	−0.04	0.01	0.22
87	145	0.15	0.08	−0.04	0.01	0.38
88	146	0.16	0.09	−0.05	0.02	0.46
89	147	0.17	0.08	−0.05	0.02	0.28
90	148	0.19	0.07	−0.05	0.02	0.02
131	189	0.10	0.08	−0.04	0.00	0.40
132	190	0.11	0.08	−0.04	0.00	0.57
133	191	0.12	0.09	−0.05	0.01	0.85
134	192	0.13	0.10	−0.05	0.01	0.83
135	193	0.14	0.10	−0.05	0.02	0.49
136	194	0.15	0.10	−0.05	0.02	0.14
<i>Z</i> = 59( <i>Pr</i> )						
85	144	0.12	0.07	−0.03	0.00	0.20

(continued on next page)

Table 2 (continued)

<i>N</i>	<i>A</i>	$\epsilon_2$	$\epsilon_3$	$\epsilon_4$	$\epsilon_6$	$\Delta E_{\epsilon_3}$ (MeV)
86	145	0.13	0.07	−0.04	0.00	0.21
87	146	0.15	0.08	−0.04	0.01	0.24
88	147	0.17	0.07	−0.05	0.02	0.26
89	148	0.19	0.05	−0.06	0.02	0.06
130	189	0.07	0.07	−0.03	0.00	0.12
131	190	0.09	0.09	−0.03	0.00	0.58
132	191	0.10	0.09	−0.04	0.00	0.75
133	192	0.11	0.10	−0.05	0.01	0.92
134	193	0.13	0.10	−0.05	0.01	0.80
135	194	0.14	0.10	−0.05	0.02	0.35
<i>Z</i> = 60( <i>Nd</i> )						
85	145	0.10	0.07	−0.02	0.00	0.10
86	146	0.14	0.06	−0.04	0.00	0.08
87	147	0.16	0.06	−0.04	0.01	0.08
88	148	0.18	0.06	−0.05	0.02	0.09
130	190	0.07	0.07	−0.03	0.00	0.14
131	191	0.09	0.09	−0.03	0.00	0.67
132	192	0.10	0.09	−0.03	0.00	0.75
133	193	0.11	0.09	−0.05	0.00	0.86
134	194	0.13	0.10	−0.05	0.01	0.64
135	195	0.14	0.10	−0.05	0.02	0.18
<i>Z</i> = 61( <i>Pm</i> )						
85	146	0.09	0.07	−0.02	0.00	0.03
86	147	0.16	0.03	−0.04	0.00	0.02
87	148	0.17	0.05	−0.04	0.01	0.06
88	149	0.19	0.04	−0.05	0.02	0.09
129	190	0.04	0.05	−0.01	0.00	0.03
130	191	0.07	0.08	−0.03	0.00	0.34
131	192	0.08	0.09	−0.03	0.00	0.82
132	193	0.10	0.09	−0.03	0.00	0.83
133	194	0.11	0.10	−0.04	0.01	0.87
134	195	0.12	0.10	−0.05	0.01	0.55
135	196	0.13	0.10	−0.05	0.01	0.05
<i>Z</i> = 62( <i>Sm</i> )						
87	149	0.17	0.03	−0.04	0.01	0.02
88	150	0.19	0.04	−0.04	0.02	0.02
89	151	0.21	0.02	−0.05	0.02	0.01
129	191	0.04	0.06	−0.01	0.00	0.09
130	192	0.07	0.08	−0.02	0.00	0.40
131	193	0.08	0.09	−0.03	0.00	0.81
132	194	0.09	0.10	−0.03	0.01	0.78
133	195	0.10	0.09	−0.04	0.00	0.79
134	196	0.12	0.10	−0.04	0.01	0.45
<i>Z</i> = 63( <i>Eu</i> )						
84	147	0.04	0.05	−0.01	0.00	0.02
129	192	0.04	0.07	−0.02	0.00	0.23
130	193	0.06	0.09	−0.02	0.00	0.54
131	194	0.07	0.10	−0.03	0.01	0.85
132	195	0.08	0.10	−0.03	0.01	0.79
133	196	0.10	0.10	−0.04	0.01	0.71
134	197	0.11	0.10	−0.05	0.01	0.36
<i>Z</i> = 64( <i>Gd</i> )						
129	193	0.04	0.07	−0.02	0.00	0.22
130	194	0.05	0.08	−0.02	0.00	0.51
131	195	0.07	0.10	−0.02	0.01	0.72
132	196	0.08	0.10	−0.03	0.01	0.64
133	197	0.10	0.09	−0.04	0.00	0.62
134	198	0.12	0.09	−0.05	0.01	0.29
<i>Z</i> = 65( <i>Tb</i> )						
128	193	0.01	0.02	0.00	0.00	0.06
129	194	0.03	0.05	−0.01	0.01	0.22
130	195	0.07	0.08	−0.03	0.00	0.44
131	196	0.07	0.10	−0.03	0.01	0.53
132	197	0.08	0.10	−0.03	0.01	0.45
133	198	0.11	0.08	−0.04	0.00	0.47
134	199	0.13	0.08	−0.05	0.01	0.17
<i>Z</i> = 66( <i>Dy</i> )						
129	195	0.03	0.06	−0.01	0.00	0.15
130	196	0.05	0.08	−0.02	0.00	0.35
131	197	0.07	0.09	−0.02	0.01	0.41
132	198	0.08	0.10	−0.02	0.01	0.29
133	199	0.11	0.08	−0.04	0.00	0.36
134	200	0.11	0.08	−0.04	0.00	0.13
<i>Z</i> = 67( <i>Ho</i> )						
129	196	0.04	0.05	−0.01	0.00	0.07
130	197	0.07	0.06	−0.02	0.00	0.17
131	198	0.07	0.09	−0.02	0.01	0.13

Table 2 (continued)

<i>N</i>	<i>A</i>	$\epsilon_2$	$\epsilon_3$	$\epsilon_4$	$\epsilon_6$	$\Delta E_{\epsilon_3}$ (MeV)
132	199	0.11	0.05	−0.04	−0.01	0.10
133	200	0.11	0.07	−0.04	0.00	0.20
134	201	0.13	0.05	−0.05	0.00	0.04
<i>Z</i> = 68( <i>Er</i> )						
129	197	0.03	0.04	−0.01	0.00	0.03
130	198	0.06	0.05	−0.02	0.00	0.10
131	199	0.07	0.08	−0.02	0.00	0.08
132	200	0.11	0.04	−0.04	−0.01	0.05
133	201	0.11	0.06	−0.04	0.00	0.16
134	202	0.11	0.06	−0.04	0.00	0.04
<i>Z</i> = 69( <i>Tm</i> )						
130	199	0.06	0.05	−0.02	0.00	0.01
133	202	0.11	0.05	−0.04	0.00	0.06
<i>Z</i> = 70( <i>Yb</i> )						
133	203	0.11	0.05	−0.04	0.00	0.04
134	204	0.11	0.04	−0.04	0.00	0.04
<i>Z</i> = 72( <i>Hf</i> )						
133	205	0.11	0.04	−0.03	−0.01	0.01
<i>Z</i> = 73( <i>Ta</i> )						
135	208	0.11	0.03	−0.03	0.00	0.08
<i>Z</i> = 74( <i>W</i> )						
135	209	0.11	0.04	−0.03	0.00	0.04
<i>Z</i> = 75( <i>Re</i> )						
135	210	0.11	0.03	−0.03	0.00	0.03
<i>Z</i> = 76( <i>Os</i> )						
134	210	0.09	0.02	−0.02	−0.01	0.02
135	211	0.11	0.04	−0.02	0.00	0.05
<i>Z</i> = 77( <i>Ir</i> )						
135	212	0.10	0.03	−0.02	−0.01	0.04
136	213	0.11	0.03	−0.02	0.00	0.02
<i>Z</i> = 78( <i>Pt</i> )						
135	213	0.09	0.04	−0.02	0.00	0.08
136	214	0.09	0.03	−0.02	0.00	0.03
137	215	0.11	0.03	−0.03	0.00	0.02
<i>Z</i> = 79( <i>Au</i> )						
135	214	0.07	0.04	−0.02	0.00	0.07
136	215	0.08	0.04	−0.02	0.00	0.08
137	216	0.09	0.04	−0.02	0.00	0.07
138	217	0.10	0.03	−0.02	0.00	0.03
<i>Z</i> = 80( <i>Hg</i> )						
135	215	0.05	0.06	−0.01	0.00	0.02
136	216	0.06	0.05	−0.01	0.00	0.02
137	217	0.07	0.06	−0.02	0.00	0.17
138	218	0.08	0.05	−0.02	0.00	0.14
139	219	0.09	0.05	−0.02	0.00	0.09
<i>Z</i> = 81( <i>Tl</i> )						
94	175	0.07	0.02	0.00	0.00	0.02
135	216	0.02	0.05	−0.01	0.00	0.05
136	217	0.03	0.06	0.00	0.00	0.06
137	218	0.05	0.06	−0.01	0.00	0.18
138	219	0.06	0.05	−0.01	0.00	0.16
139	220	0.07	0.06	−0.01	0.01	0.24
140	221	0.07	0.05	−0.01	0.00	0.13
<i>Z</i> = 82( <i>Pb</i> )						
97	179	0.01	0.04	0.00	0.00	0.04
98	180	0.00	0.03	0.00	0.00	0.02
99	181	0.02	0.03	0.00	0.00	0.10
100	182	0.01	0.02	0.00	0.00	0.08
101	183	−0.01	0.04	−0.01	0.00	0.06
102	184	0.00	0.02	−0.01	0.00	0.04
134	216	0.01	0.04	0.00	0.00	0.02
135	217	0.02	0.07	−0.01	0.01	0.16
136	218	0.01	0.06	0.00	0.00	0.16
137	219	0.03	0.07	−0.01	0.00	0.25
138	220	0.01	0.07	−0.01	0.00	0.23
139	221	0.03	0.07	−0.01	0.01	0.34
140	222	0.01	0.07	0.00	0.01	0.26
<i>Z</i> = 83( <i>Bi</i> )						
95	178	0.07	0.07	−0.01	0.00	0.20
96	179	0.07	0.07	−0.01	0.00	0.09
97	180	0.05	0.07	−0.01	0.00	0.10
133	216	0.04	0.09	−0.02	0.00	0.12
134	217	0.04	0.08	−0.02	0.00	0.16
135	218	0.05	0.08	−0.02	0.00	0.32
136	219	0.05	0.08	−0.02	0.00	0.25
137	220	0.07	0.08	−0.03	0.00	0.38

Table 2 (continued)

N	A	$\epsilon_2$	$\epsilon_3$	$\epsilon_4$	$\epsilon_6$	$\Delta E_{\epsilon_3}$ (MeV)
138	221	0.08	0.08	−0.03	0.00	0.28
139	222	0.09	0.07	−0.03	0.00	0.10
Z = 84(Po)						
133	217	0.04	0.09	−0.02	0.00	0.34
134	218	0.05	0.09	−0.02	0.00	0.44
135	219	0.08	0.08	−0.04	0.00	0.46
136	220	0.09	0.09	−0.04	0.00	0.42
137	221	0.09	0.09	−0.04	0.00	0.32
138	222	0.10	0.08	−0.04	0.00	0.16
Z = 85(At)						
131	216	0.05	0.09	−0.03	0.00	0.29
132	217	0.06	0.10	−0.03	0.00	0.53
133	218	0.08	0.10	−0.04	0.00	0.65
134	219	0.09	0.09	−0.05	−0.01	0.64
135	220	0.10	0.09	−0.05	0.00	0.74
136	221	0.10	0.09	−0.05	0.00	0.63
137	222	0.10	0.09	−0.05	0.00	0.41
138	223	0.11	0.08	−0.05	0.01	0.24
Z = 85(At)						
139	224	0.13	0.04	−0.07	−0.01	0.07
140	225	0.14	0.02	−0.07	−0.01	0.03
141	226	0.15	0.02	−0.07	0.00	0.03
Z = 86(Rn)						
131	217	0.06	0.10	−0.03	0.00	0.59
132	218	0.07	0.10	−0.04	0.00	0.67
133	219	0.09	0.09	−0.05	−0.01	0.85
134	220	0.10	0.09	−0.05	0.00	0.85
135	221	0.10	0.09	−0.05	0.00	0.82
136	222	0.10	0.09	−0.05	0.00	0.64
137	223	0.13	0.09	−0.06	0.00	0.47
138	224	0.13	0.08	−0.06	0.00	0.29
139	225	0.15	0.05	−0.07	0.00	0.12
140	226	0.15	0.04	−0.07	0.00	0.09
141	227	0.16	0.02	−0.07	0.00	0.03
146	232	0.21	0.02	−0.05	0.03	0.02
Z = 87(Fr)						
130	217	0.07	0.09	−0.04	−0.01	0.34
131	218	0.08	0.10	−0.04	0.00	1.20
132	219	0.09	0.10	−0.05	0.00	1.04
133	220	0.10	0.09	−0.06	−0.01	1.20
134	221	0.10	0.10	−0.06	0.00	1.14
135	222	0.11	0.10	−0.06	0.00	1.05
136	223	0.12	0.10	−0.06	0.01	0.90
137	224	0.13	0.10	−0.06	0.01	0.67
138	225	0.14	0.09	−0.06	0.01	0.41
139	226	0.15	0.06	−0.07	0.00	0.22
140	227	0.15	0.05	−0.07	0.00	0.13
141	228	0.16	0.03	−0.07	0.00	0.06
Z = 88(Ra)						
129	217	0.05	0.08	−0.03	0.00	0.13
130	218	0.07	0.09	−0.04	0.00	0.59
131	219	0.08	0.10	−0.04	0.00	1.06
132	220	0.10	0.09	−0.06	−0.01	1.20
133	221	0.10	0.10	−0.06	0.00	1.35
134	222	0.11	0.10	−0.06	0.00	1.27
135	223	0.12	0.10	−0.06	0.01	1.17
136	224	0.13	0.10	−0.06	0.01	0.91
137	225	0.14	0.10	−0.06	0.01	0.63
138	226	0.15	0.08	−0.07	0.01	0.40
139	227	0.16	0.07	−0.07	0.01	0.20
140	228	0.16	0.06	−0.07	0.01	0.08
141	229	0.17	0.02	−0.08	0.01	0.03
Z = 89(Ac)						
129	218	0.07	0.09	−0.04	0.00	0.58
130	219	0.08	0.10	−0.04	0.00	1.18
131	220	0.09	0.10	−0.05	0.00	1.28
132	221	0.10	0.10	−0.05	0.00	1.42
133	222	0.11	0.10	−0.06	0.00	1.43
134	223	0.12	0.10	−0.06	0.00	1.39
135	224	0.13	0.11	−0.06	0.01	1.16
136	225	0.13	0.10	−0.06	0.01	0.78
137	226	0.14	0.10	−0.06	0.01	0.49
138	227	0.15	0.08	−0.07	0.01	0.33
139	228	0.16	0.07	−0.07	0.01	0.13
Z = 90(Th)						
129	219	0.07	0.09	−0.03	0.00	0.72
130	220	0.08	0.10	−0.04	0.00	1.33

Table 2 (continued)

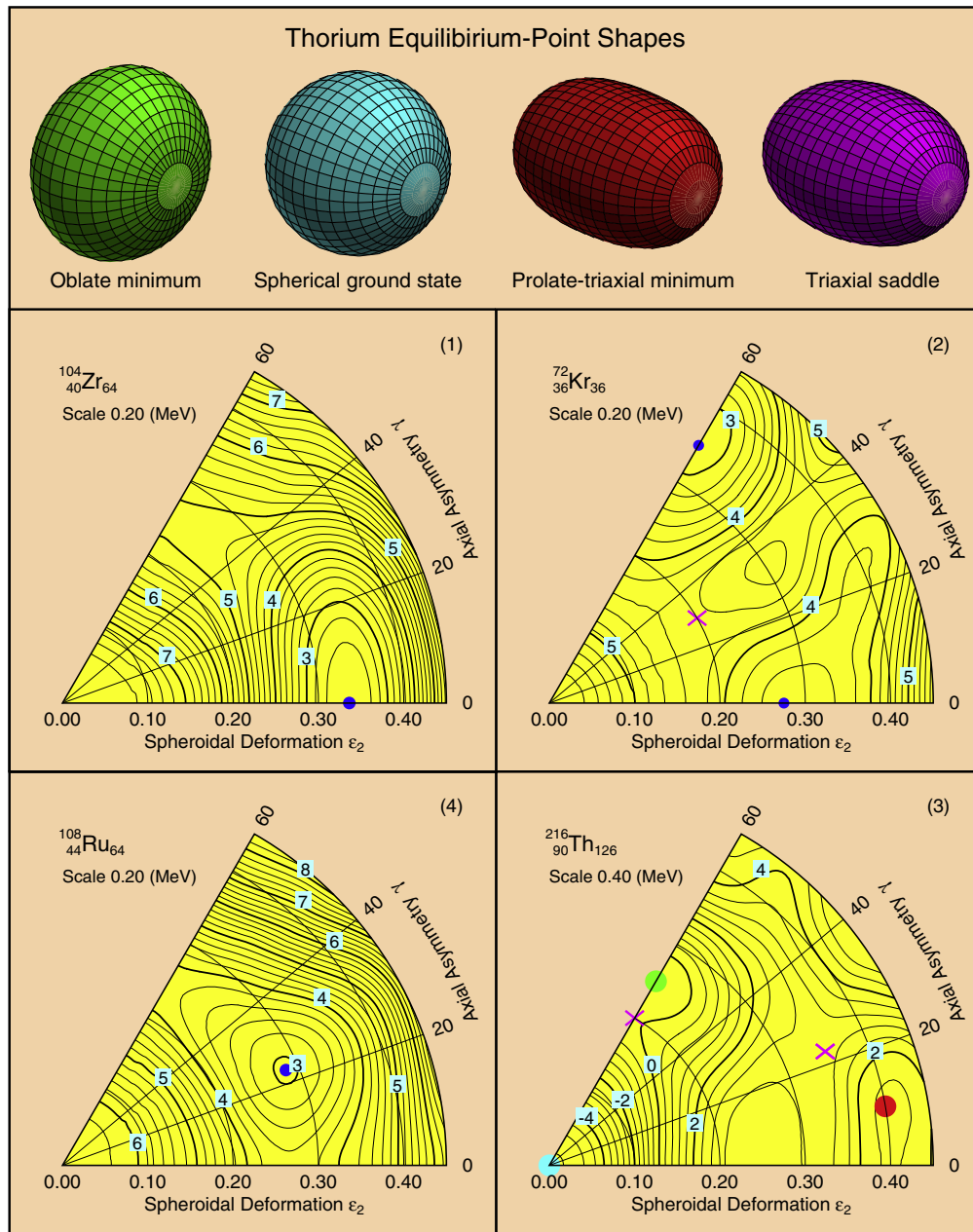
N	A	$\epsilon_2$	$\epsilon_3$	$\epsilon_4$	$\epsilon_6$	$\Delta E_{\epsilon_3}$ (MeV)
131	221	0.10	0.09	−0.05	0.00	1.31
132	222	0.10	0.10	−0.05	0.00	1.35
133	223	0.12	0.10	−0.06	0.00	1.42
134	224	0.13	0.11	−0.06	0.01	1.22
135	225	0.13	0.10	−0.06	0.01	0.91
136	226	0.14	0.10	−0.06	0.01	0.50
137	227	0.15	0.10	−0.06	0.02	0.27
138	228	0.16	0.08	−0.07	0.01	0.08
Z = 91(Pa)						
129	220	0.08	0.09	−0.04	0.00	1.14
130	221	0.09	0.10	−0.04	0.00	1.29
131	222	0.10	0.09	−0.05	0.00	1.38
132	223	0.11	0.10	−0.05	0.00	1.36
133	224	0.12	0.10	−0.06	0.01	1.35
134	225	0.13	0.11	−0.06	0.01	0.99
135	226	0.14	0.11	−0.06	0.02	0.61
136	227	0.14	0.10	−0.06	0.02	0.27
137	228	0.15	0.10	−0.06	0.02	0.04
Z = 92(U)						
127	219	0.02	0.04	−0.01	0.00	0.04
128	220	0.05	0.08	−0.02	0.00	0.08
129	221	0.08	0.09	−0.03	0.00	1.16
130	222	0.09	0.10	−0.04	0.01	1.21
131	223	0.10	0.10	−0.04	0.01	1.27
132	224	0.12	0.10	−0.05	0.01	1.22
133	225	0.13	0.10	−0.06	0.01	1.06
134	226	0.13	0.10	−0.06	0.01	0.60
135	227	0.14	0.10	−0.06	0.02	0.30
Z = 93(Np)						
127	220	0.03	0.06	−0.01	0.00	0.22
128	221	0.05	0.08	−0.02	0.00	0.48
129	222	0.08	0.09	−0.03	0.00	1.21
130	223	0.09	0.10	−0.03	0.01	1.19
131	224	0.10	0.11	−0.03	0.01	1.23
132	225	0.12	0.10	−0.05	0.01	0.87
133	226	0.13	0.09	−0.06	0.01	0.63
134	227	0.14	0.10	−0.06	0.02	0.23
135	228	0.15	0.10	−0.06	0.02	0.01
Z = 94(Pu)						
127	221	0.03	0.06	−0.01	0.00	0.21
128	222	0.05	0.08	−0.02	0.00	0.35
129	223	0.07	0.09	−0.02	0.00	1.14
130	224	0.09	0.10	−0.03	0.01	1.09
131	225	0.10	0.11	−0.03	0.01	0.94
132	226	0.12	0.10	−0.05	0.01	0.59
133	227	0.13	0.10	−0.05	0.01	0.48
134	228	0.14	0.10	−0.05	0.01	0.04
Z = 95(Am)						
125	220	0.01	0.03	0.00	0.00	0.06
126	221	0.01	0.04	0.00	0.00	0.11
127	222	0.04	0.07	−0.01	0.00	0.44
128	223	0.05	0.08	−0.01	0.00	0.68
129	224	0.07	0.10	−0.02	0.01	1.14
130	225	0.09	0.10	−0.03	0.01	0.95
131	226	0.10	0.11	−0.03	0.01	0.57
132	227	0.12	0.10	−0.04	0.01	0.21
133	228	0.14	0.09	−0.05	0.01	0.11
Z = 96(Cm)						
125	221	0.02	0.03	0.00	0.00	0.01
126	222	0.00	0.03	0.00	0.00	0.02
128	224	0.04	0.08	−0.01	0.00	0.52
129	225	0.06	0.09	−0.02	0.01	1.08
130	226	0.08	0.10	−0.03	0.01	0.84
131	227	0.09	0.11	−0.03	0.01	0.43
132	228	0.14	0.08	−0.05	0.01	0.02
Z = 97(Bk)						
125	222	0.03	0.04	0.00	0.00	0.07
126	223	0.01	0.05	0.00	0.00	0.14
127	224	0.03	0.07	−0.01	0.00	0.55
128	225	0.04	0.08	−0.01	0.00	0.75
129	226	0.06	0.10	−0.02	0.01	0.87
130	227	0.08	0.10	−0.02	0.01	0.31
131	228	0.09	0.11	−0.03	0.01	0.01
Z = 98(Cf)						
125	223	0.03	0.04	0.00	0.00	0.04
126	224	0.00	0.05	0.00	0.00	0.10

(continued on next page)

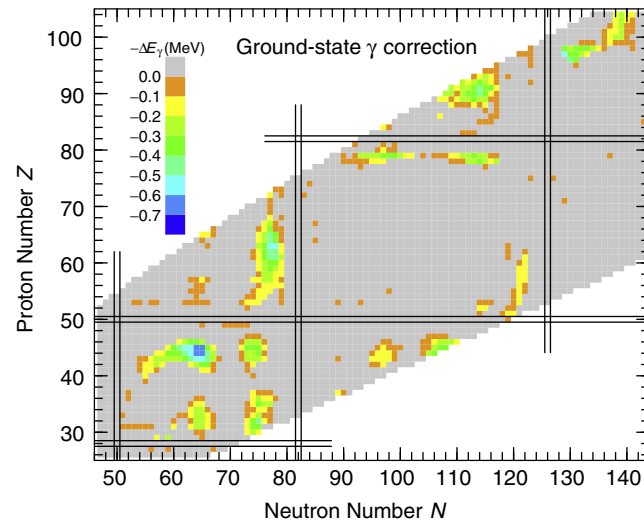


**Table 2** (continued)

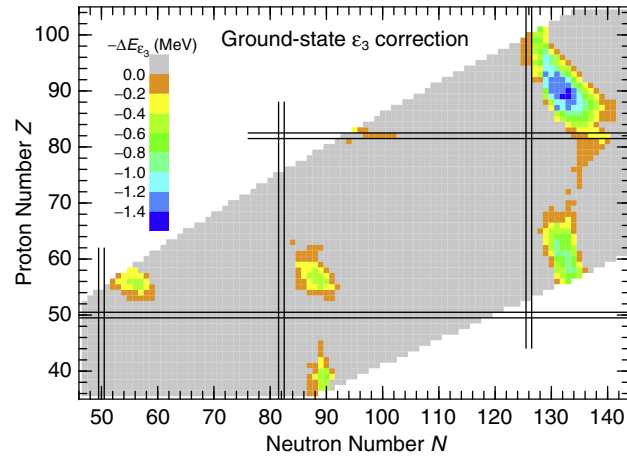
$N$	$A$	$\epsilon_2$	$\epsilon_3$	$\epsilon_4$	$\epsilon_6$	$\Delta E_{\epsilon_3}$ (MeV)
127	225	0.03	0.07	−0.01	0.00	0.47
128	226	0.03	0.08	−0.01	0.01	0.56
129	227	0.05	0.09	−0.01	0.01	0.68
130	228	0.07	0.10	−0.02	0.01	0.06
$Z = 99(\text{Es})$						
125	224	0.01	0.05	0.00	0.00	0.13
126	225	0.00	0.06	0.00	0.00	0.20
127	226	0.02	0.07	−0.01	0.00	0.61
128	227	0.03	0.08	−0.01	0.01	0.71
129	228	0.04	0.09	−0.01	0.01	0.21
$Z = 100(\text{Fm})$						
126	226	0.00	0.06	0.00	0.00	0.12
127	227	0.01	0.07	−0.01	0.00	0.47
128	228	0.02	0.08	−0.01	0.01	0.52
129	229	0.04	0.09	−0.01	0.01	0.28
$Z = 101(\text{Md})$						
128	229	0.01	0.08	−0.01	0.00	0.61
129	230	0.02	0.09	−0.01	0.01	0.23



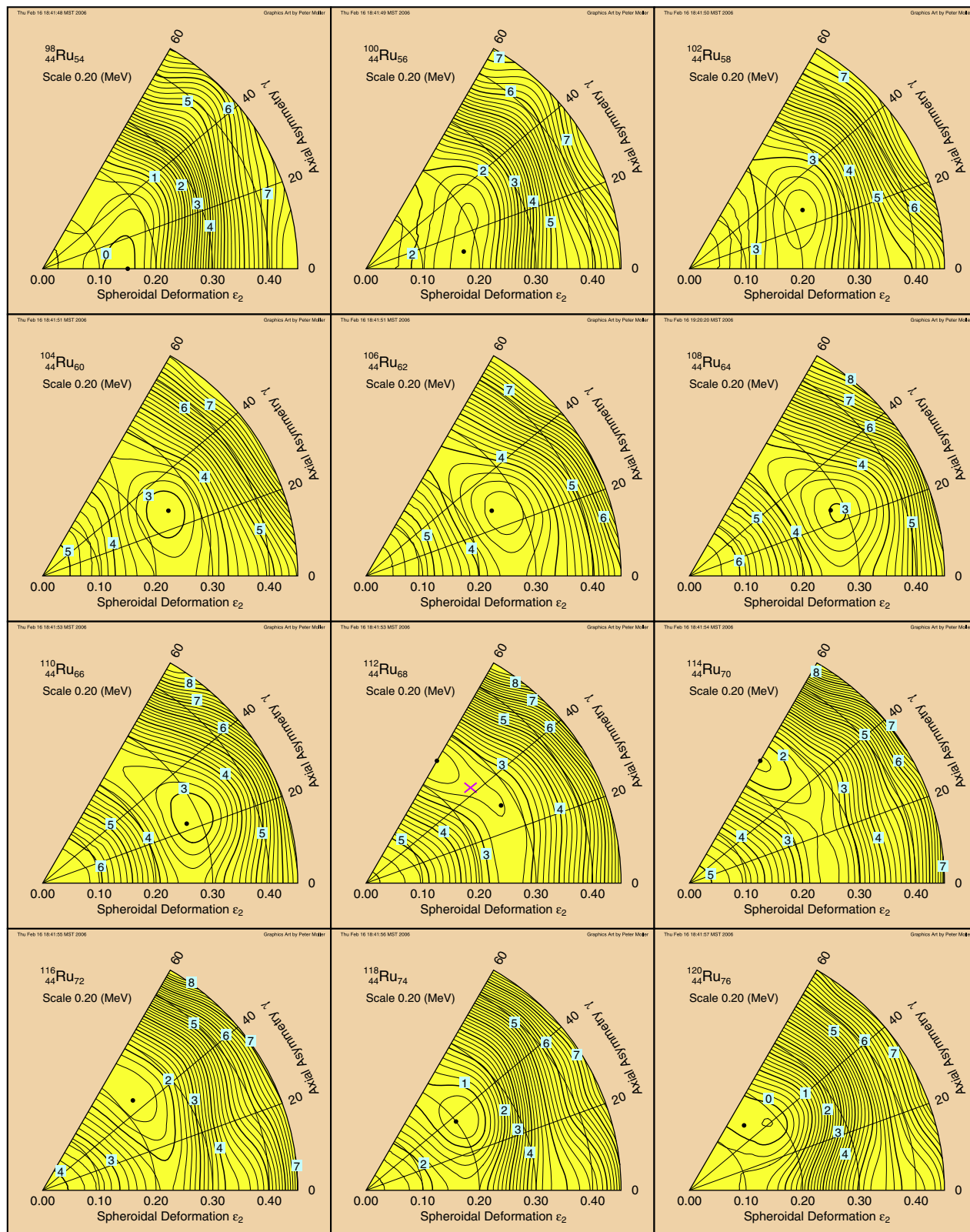
**Graph 1.** Four calculated potential-energy surfaces versus  $\epsilon_2$  and  $\gamma$  (minimized with respect to  $\epsilon_4$ ).



**Graph 2.** Calculated ground-state axial-asymmetry instability for nuclei in the range  $47 < N < 143$ .



**Graph 3.** Calculated ground-state octupole instability for nuclei in the range  $47 < N < 143$ .



**Graph 4.** Twelve calculated potential-energy surfaces versus  $\epsilon_2$  and  $\gamma$  (minimized with respect to  $\epsilon_4$ ) for even Ru isotopes from  $^{98}\text{Ru}$  to  $^{120}\text{Ru}$ .